IEEE Access
Multidisciplinary | Rapid Review | Open Access Journal

Received January 16, 2017, accepted February 2, 2017, date of publication March 23, 2017, date of current version May 17, 2017.

*Digital Object Identifier 10.1109/ACCESS.2017.2685592*

# A Risk-Informed Interference Assessment of MetSat/LTE Coexistence

**J. PIERRE DE VRIES[1], URI LIVNAT[2], AND SUSAN P. TONKIN[3]**
[1]Silicon Flatirons Center, University of Colorado Law School, Boulder, CO 80309 USA
[2]Nokia, Cambridge, MA 02142 USA
[3]Independent Researcher, Kirkland, WA 98033 USA

Corresponding author: S. P. Tonkin (stonkin@brightwave.com)

**ABSTRACT** Quantitative risk assessment has recently been proposed to assess the impact of a new radio service allocation on incumbents. This paper demonstrates its viability by performing a risk-informed interference assessment in a recent U.S. case: the protection of meteorological satellite earth stations from interference by cellular mobile transmitters. We find that the hazard selected by policy makers (co-channel interference with the receiving antenna at 5° elevation) was not the most severe, and that their worst case approach overlooked more significant risks, notably adjacent band interference. We begin with an inventory of the performance hazards. We survey consequence metrics that quantify the severity of interference, and select the interference protection criteria defined in Recommendation ITU-R SA.1026-4. We then use Monte Carlo modeling to calculate probability distributions of resulting interference due to co-channel and adjacent band transmissions. We identify a co-channel exclusion distance that keeps interference risk below the SA.1026-4 criteria. We show that the binding constraint is not the ITU-R ''long-term'' interference mode (5° antenna elevation), but rather the ''short-term'' interference when the elevation is 13°. We give an extensive sensitivity analysis showing that the propagation modeling, and particularly the choice of clutter model, can have a significant effect on the results. We conclude that quantitative risk assessment yields useful insights for analyzing coexistence. Protection criteria that combine an interfering power level with statistical exceedance limits were essential to our analysis, and we recommend that policy makers adopt statistical service rules more widely to support future risk analysis. Our analysis was limited by the unavailability of baseline values for service metrics, and the lack of transparency in previous studies, notably ITU-R recommendations. We recommend that regulators encourage parties to provide baseline values and the methods underlying interference criteria and coexistence assessments.

**INDEX TERMS** Cellular phones, clutter, governmental factors, interference, mobile communication, Monte Carlo methods, risk analysis, satellite communication, satellite ground stations.

## I. INTRODUCTION

Probabilistic risk assessment has been proposed as a way to improve analysis of the harm that may be caused by changes in radio service rules by considering the ''risk triplet'' rather than the worst case [1], [2]: What can happen, how likely is it, and what are the consequences?

This paper demonstrates the viability of this approach and the insights it can provide by analyzing a case study introduced by De Vries [3], [4]: the protection of meteorological satellite (MetSat) services from cellular systems.

Reference [1] defined *risk-informed interference assessment* as the systematic, quantitative analysis of the likelihood and consequence of interference hazards caused by the interaction between radio systems, especially incumbent and prospective radio service. The likelihoods and consequences of hazards are often plotted on a *risk chart*; Fig. 1 shows a generic version.

In this paper, we provide the first journal publication of a detailed risk-informed interference assessment. We use Monte Carlo modeling to calculate probability distributions of aggregate interference due to co-channel and adjacent band transmissions, and to identify exclusion distances. We extend the calculations in [5] by providing additional statistical analysis and aggregating co-channel and adjacent band hazards; develop quantitative versions of the risk chart; add a sensitivity analysis; and show that the results cast doubt on the results in [6] and [7] that underpin the current FCC rules for cellular sharing of the MetSat band.

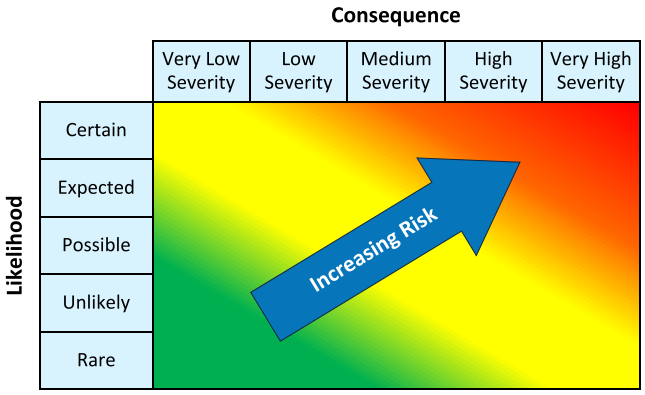


**FIGURE 1.** A qualitative, generic risk chart.

Section II gives an overview of the case study. The analysis is divided into four elements, following [3]: 1) Make an inventory of all significant harmful interference hazard modes; 2) define a consequence metric to characterize the severity of hazards; 3) assess the likelihood and consequence of each hazard mode; 4) aggregate the results.

We discuss the four elements in Sections II through VI and show how they can be used to inform decision making. Section VII identifies potential further work. Section VIII provides a sensitivity analysis. Section IX gives general conclusions and recommendations.

## II. METSAT/LTE CASE

This section describes the services in our case study. We selected the MetSat/LTE case because earlier studies by the National Telecommunications Information Administration (NTIA) generated an extensive consensus record of interference parameters and analysis [6], [7].

### A. REGULATORY BACKGROUND

The NTIA first studied coexistence between federal and commercial services to determine whether 115 MHz of spectrum currently used by Federal agencies could be made available for wireless broadband [6]. The Commerce Spectrum Management Advisory Committee's Working Group 1 (CSMAC WG1) was tasked with making more detailed recommendations, resulting in significant regulatory advances [7]. The exclusion zones (areas where LTE mobiles would not be allowed to operate) defined in [6] were converted to protection zones (areas within which LTE mobiles could be used with the approval of MetSat operators), and their radii were reduced by 21–89% [7]. Based on this work, the 1695–1710 MHz band was included in the Federal Communication Commission (FCC) 2015 AWS-3 auction 97 [8]. This band was already in use by MetSat receiving earth stations, and it was necessary to protect the MetSat earth stations from harmful interference from the proposed cellular mobile devices.

While this work builds on [6], [7], it has different goals and methods. First, the purpose of this case study is to illustrate the method of risk-informed interference assessment, not to inform service rules acceptable to both federal and commercial parties that would lead to prompt reallocation and auctioning of the band. Second, both [6] and [7] used a fixed interference-to-noise ($I/N$) criterion of $-10$ dB for acceptable interference, whereas this study uses the interfering signal power and not-to-exceed time percentage parameters defined in [9].

Third, [6] and [7] calculated interference using the Irregular Terrain Model (ITM) for propagation, whereas we analyze a generic site using an empirical, area-general propagation model (Extended Hata). Fourth, [6] and [7] used a largely deterministic, extreme value approach (i.e. single values for most interference parameters), with the exception that [7] used a probability distribution for mobile transmit power. In contrast, this study uses quantitative risk analysis based on probability distributions for as many variables as possible.

### B. METSAT EARTH STATION AND LTE MOBILE TRANSMITTER CHARACTERISTICS

The services to be protected are satellite earth stations receiving imagery and other data from four geostationary and six polar-orbiting satellites, six platforms in the polar-orbiting Defense Meteorological Satellite Program (DMSP), and the Jason-2 Altimetry satellite (note that DMSP and Jason-2 are not discussed in [7]).

This case study deals with the reception of signals from Polar-orbiting Operational Environmental Satellites (POES, although the protection of geostationary satellite services (GOES) would be part of a complete analysis. We selected POES because [7] showed that it was more susceptible to LTE interference than GOES. The basic characteristics of the POES system are described in [10]. Fig. 2(a) and Fig. 2(b), taken from [11], illustrate the POES orbits; Fig. 2(c) shows a typical earth station antenna [12].

The potentially interfering systems we consider are LTE cellular mobile transmitters (LTE mobiles) operating in the AWS-3 band; see Fig. 3, based on [13]. We assume that this service is deployed as separate 5 MHz and 10 MHz license blocks. We focus our analysis on interference in the upper 1700–1710 MHz B1 block, which overlaps with the 1702.5 and 1707 MHz POES reception frequencies.

## III. FIRST ELEMENT: MAKE AN INVENTORY OF HAZARDS

The first step in probabilistic risk assessment is to make an inventory of all expected hazards, that is, phenomena that could cause harm.

### A. HAZARDS

Table 1 summarizes the hazards. We only model interference from known, intentional radiators. We leave aside interference due to intermodulation products and spurious emissions, and ignore the risk of intentional jamming.

#### 1) NON-INTERFERENCE HAZARDS

Radio interference is not the only hazard to the reception of satellite signals. Two general categories are faults and failures, and degradation of the desired signal strength. Since

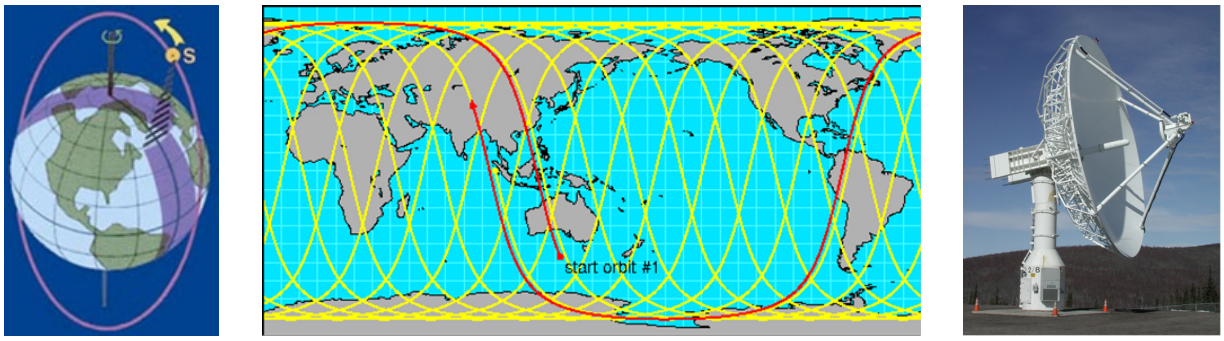


(a) (b) (c)

**FIGURE 2.** Polar Orbital Exploration Satellite (POES) system elements. A high gain dish antenna is needed because the received signal at the ground is very weak. (a) Example of a near-polar orbit. (b) Polar orbit ground track for 24 hours. (c) 13 meter POES antenna.

**TABLE 1.** Examples of performance hazards to MetSat reception.

| | | Persistent (long-term) | Intermittent (short-term) |
|---|---|---|---|
| Non-interference hazards | | System failure, satellite or receiver failure, operator error, power outage<br>Signal strength loss e.g. due to ionospheric scintillation | Power supply spikes |
| Co-channel interferers | | Persistent weak interference from co-channel operators combined with occasional fading of the satellite signal | Short-term, strong interference that can overwhelm a persistent strong desired signal |
| Frequency-adjacent interferers | Out of band emissions (OOBE) | Spillover from transmissions by AWS-1 mobiles not fully excluded from MetSat channel due to limited AWS-1 adjacent channel filtering | Same |
| | Adjacent band interference (ABI) | Power in AWS-1 band not fully excluded by MetSat adjacent channel selectivity (ACS) | Same |
| | Intermodulation and spurious emissions | Interference in MetSat channel due to intermodulation of transmissions in adjacent bands | Interference spikes due to spurious emissions |

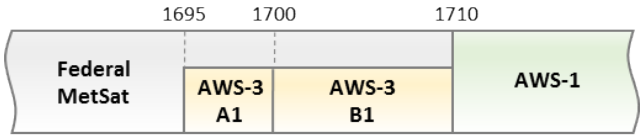


**FIGURE 3.** AWS-3 blocks in 1695–1710 MHz.

we have not been able to obtain data on the incidence or severity of these hazards, they are not included in the numerical analysis.

Faults and failures include system and device failures (terrestrial or in orbit), device misconfiguration and degradation, physical phenomena, power outages, and operator error. Physical phenomena include mounting stresses (e.g. bending and twisting), electrical static, shock, vibration, temperature and humidity extremes, condensation, liquids, salt spray, conductive dusts, mold growth, oxidation, corrosion, abrasion, and so on.

The desired satellite signal can be degraded by attenuation between the satellite and the earth station, e.g., through ionospheric scintillation, a rapid fluctuation of radio-frequency signal phase and/or amplitude generated as a signal passes through the ionosphere. Ionospheric scintillation is a well-known phenomenon that has been studied extensively, in part because it also affects GPS signals. (Conveniently, the commonly used GPS L1 frequency 1575.42 MHz is moderately close to the band of interest in this study.) It is primarily an equatorial and high-latitude ionospheric phenomenon, although it can occur at lower intensity at all latitudes. We suspect it is unlikely to play a role in MetSat reception except in Guam, Hawaii, and perhaps Alaska.

### 2) CO-CHANNEL INTERFERENCE

The canonical analysis of interference to MetSat systems, Recommendation SA.1026-4 [9] of the International Telecommunication Union, Radiocommunication Sector (ITUR), only considers co-channel interference. Reference [9] provides long- and short-term interference protection criteria (IPC), defined as the interfering signal power in the reference bandwidth to be exceeded no more than 20% and 0.0125% of the time, respectively.

As outlined in [13], over the long term, fading of the satellite signal combines with relatively low interference levels to cause outage. Short-term bursts of higher interference can

occasionally combine with nominal satellite signals to cause outage.

Reference [9] uses different earth station antenna elevation angles to calculate the long- and short-term criteria; for the service at issue in this study, 5° and 13°, respectively. The long-term interference levels are lower (i.e., more stringent) than the short-term levels. We model both in Section VIII.

#### 3) INTERFERENCE FROM TRANSMITTERS IN ADJACENT BANDS

Neither [6], [7], nor [9] addresses adjacent band interference. We assume that the long- and short-term interference protection scenarios defined for the co-channel transmissions also apply in this case.

The most likely current source of intentionally radiated harmful interference is cellular mobiles transmitting in the adjacent AWS-1 band, for which there is no exclusion zone; an interfering mobile can be right next to an earth station receiver. The closest cellular mobiles in frequency are in the AWS-1 A block, 1710–1720 MHz.

There are two main ways an AWS-1 mobile could interfere with a MetSat receiver: a small part of its power is radiated or ''leaked'' in the adjacent MetSat passband, OOBE; or imperfect filtering in the MetSat receiver admits some of the energy radiated within the AWS-1 band, ABI. We model both mechanisms in Section V.C.

### B. DETERMINANTS OF INTERFERENCE

The interaction between two radio systems is determined by the characteristics of the systems' transmitters and receivers, and the coupling between them due to factors such as antenna gain patterns and path loss.

The key interference parameters for the MetSat/LTE case, and the values used in our modeling, are given in Table 2 below.

#### 1) TRANSMITTER CHARACTERISTICS

The amount of power transmitted by an interfering LTE mobile is key to determining the amount of interference experienced by a receiver.

We use the cumulative distribution function (CDF) of LTE mobile EIRP published in [7, Appendix 3-3]. The transmit power varies, with median values −13 dBm and −3 dBm for the suburban and rural cases, respectively, and a maximum of +20 dBm. This distribution was calculated on the worst-case assumption that every base station is fully loaded, and that all mobiles have their buffers full at all times [7]. Since the critical time window for POES operation is only a few tens of seconds, however, it seems to be a reasonable default in the absence of data from cellular operators on the statistics of cell loading.

Another important consideration is the location of transmitters. We follow [7] in assuming a homogenous, isotropic hexagonal cell structure with 18 mobiles per 10 MHz channel associated with each base station (see Section V.A). This is evidently not a real-world deployment pattern, but is appropriate for a generic, non-site-specific analysis such as this.

#### 2) RECEIVER CHARACTERISTICS

In most interference analyses—for example, in TV reception—the characteristics of individual receivers deployed in a service vary and their locations may be unknown. Matters are greatly simplified in our case study because the affected MetSat receivers are a small, well-defined population with known characteristics and locations [6, Appendix A].

For the purposes of this exercise we assume a receiver with a typical but relatively conservative (i.e., low) earth station antenna gain of 30 dBi, and the weakest adjacent channel selectivity (−60 dB at ±12.0 MHz) from those listed in [6]. POES satellites provide several different data feeds [10]. We model the HRPT service since it is the highest bandwidth service, and thus most susceptible to interference. We use the receiver system noise temperature specified for the HRPT service in [9, Table 2] and the antenna model given in ITU-R F.1245-2.

Since the 1.5 MHz LTE mobile channel is wider than the 1.33 MHz MetSat receiver channel, not all the power transmitted by the mobile that overlaps the MetSat channel is admitted to the receiver. The reduction in power is quantified by the OTR [7, Appendix 7, eq. (12)], which is 0.5 dB for this ratio of emission bandwidth and receiver selectivity.

Following [7], we subtract 1 dB for additional losses associated with MetSat receiver insertion loss, cable loss, polarization mismatch loss, etc.

#### 3) TRANSMITTER-RECEIVER COUPLING

The two main factors influencing the coupling between interfering transmitters and affected receivers are the attenuation of transmitted energy along the paths between them (termed path loss or propagation loss), and the performance of the antennas at the two endpoints.

We use the Extended Hata propagation model developed by the NTIA for 3.5 GHz exclusion zone analysis [15, Sec. 4.7 and Appendix A] to calculate the median path loss between individual mobiles and the MetSat receiver. This model is commonly used in cellular deployment studies and accounts reasonably well for the suburban clutter expected around a MetSat receiver [15].

Uncertainty about the path loss between transmitters and the receiver leads to uncertainty in the amount of interfering power. There are broadly speaking two kinds of propagation uncertainty: differences in path loss as the transmitter moves about in time, position, or frequency in a limited region, sometimes called fading and referred to in this document as location variability; and differences between the predictions of different propagation models.

Location variability is often modeled by adding a zero-mean random variable to the median path loss; we use a log-normal distribution with 8 dB standard deviation (cf. [15, Table A−1]). We ignore fast fading, following [6], [7]. We also ignore body loss, i.e. attenuation of the LTE mobile signal due to transmission through the user's body, as a conservative assumption.

**TABLE 2. Interference parameter values used in modeling.**

| Parameter | Value(s) | Characteristics in this study | Areas for improvement |
|---|---|---|---|
| *Transmitter characteristics* | | | |
| LTE mobile uplink total Equivalent Isotropic Radiated Power (EIRP) per device | Probability distribution for suburban and rural EIRP; values range from 20 dBm to -30 dBm ([7, Appendix 3]). | Probability distribution | Use distributions of system loading and traffic buffers to calculate distribution |
| Channel width | Nominal 10 MHz channel; only 9 MHz used, per 3GPP. | Fixed, single value | Study effects of 5 and 15 MHz channels |
| LTE mobile uplink instantaneous channel loading | Fixed, 100%, using assumption in [7]. | Fixed, worst case | Use distributions for system loading and traffic model |
| LTE cellular deployment | Assume hexagonal cell sites with different inter-site distance for suburban (1.732 km) and rural (7 km) deployment [7, Appendix 7]. This leads to base station densities of 0.386 /km$^2$ (suburban) and 0.024 /km$^2$ (rural). Circular suburban/rural boundary at 30 km from MetSat receiver. | Fixed, site general | Place base stations following actual population density in site-specific model |
| LTE mobile location, density | Randomly distributed based on base station densities. 18 mobiles per base station for 10 MHz channel. Reference [7, Appendix 3] implies 1.16 mobiles/km$^2$ (suburban) and 0.071 mobiles/km$^2$ (rural). For co-channel, sample 3 of the 18 (i.e. one per 10 MHz sector). | Random location<br>Fixed density | Use probability distribution for number of mobiles per base station |
| LTE mobile antenna height | 1.5 m for all cases. | Fixed, typical | |
| LTE mobile antenna gain | 0 dBi (values in the field typically order -4 to -8 dBi). | Fixed, worst case | Use distribution of antenna gains reflecting fielded devices |
| Mobile out of band emissions (OOBE) | Adjacent channel leakage ratio (ACLR) uniformly distributed from 30-40 dB. | Probability distribution; varied in sensitivity analysis | |
| *Receiver characteristics* | | | |
| Satellite orbit and service | POES, High Resolution Picture Transmission (HRPT) service. | Probability distribution | Add other POES services; model GOES receivers |
| Center frequency (MHz) | 1707 MHz; nearest AWS-1 band (POES also transmits at 1698 and 1702.5 MHz). | Fixed, single value | Model interference to all three frequencies |
| Receiver center frequency, 3 dB bandwidth, noise figure | 1.33 MHz (representative value, based on [6, Appendix A]. | Fixed, worst case | |
| Frequency dependent rejection (dB) | On-tune rejection (OTR) 0.5 dB = 10log(1.5 MHz/1.33 MHz); off-frequency rejection not computed. | Fixed, site general | |
| Receiver selectivity (relative attenuation as a function of frequency offset) | -3 dB @ ± 0.665 MHz<br>-20 dB @ ± 1.34 MHz<br>-60 dB @ ± 12.0 MHz<br>(least selective receiver, [6, Table A-5] ). | Random location<br>Fixed density | |
| Receiver system noise temperature | 5° elevation: 320 K<br>13° elevation: 210 K<br>(based on [9, Table 2] for HRPT). | Fixed, typical | |
| Main beam antenna gain of receiver (dBi) | 30 dBi (most typical, also smallest reported in [6, Appendix A]). | Fixed, worst case | |
| Antenna model | Azimuth and elevation gain relative to main beam direction, using ITU-R F.1245-2. | Probability distribution; varied in sensitivity analysis | |
| Elevation angle | Per [9, Table 2] for HRPT:<br>Long-term protection: 5°<br>Short-term protection: 13°. | Probability distribution | |
| Antenna height above local terrain | 20 m (representative value, based on [6, Appendix A]). | Fixed, single value | |
| Azimuth | Not specified since using an area-general model. | Fixed, worst case | |

**TABLE 2.** ***Continued.*** **Interference parameter values used in modeling.**

| Parameter | Value(s) | Characteristics in this study | Areas for improvement |
|---|---|---|---|
| *Transmitter-Receiver Coupling* | | | |
| Path loss (dB) | Area general model:<br>1 km and beyond: Extended Hata with suburban clutter [15].<br>20 m to 1 km: interpolation between free space at 20 m and Extended Hata at 1 km. | Probability distribution;<br>ITM and different clutter models included in sensitivity analysis | |
| Location variability | 1 km and beyond: log-normal distribution, zero-mean, 8 dB standard deviation.<br>20 m to 1 km: interpolation between 0 dB and 8 dB standard deviation. | Probability distribution;<br>standard deviation varied in sensitivity analysis | |
| Body loss at mobile | 0 dB. | Fixed, worst case | Use probability distributions for body loss |
| Additional losses (dB) | Receiver insertion loss, cable loss, polarization mismatch loss, etc. Fixed, 1 dB [7, Appendix 7]. | Fixed | |

Differences between propagation models and their parameters lead to systematic differences in the predicted path loss. We explore variations of the Extended Hata model together with the ITM propagation model in our sensitivity analysis, Section VIII.

Turning to antenna effects, cellular mobiles are assumed to be radiating uniformly in all directions, i.e. 0 dBi mobile antenna gain. In contrast, MetSat earth station antennas are highly directional, with the 30-40 dBi maximum gain along the main beam direction. The antennas follow satellites across the sky as they appear over the horizon, rise towards the meridian, and then set. Since the interfering transmitters are at ground level, the maximum coupling (and thus maximum interference) occurs when the earth station antenna is at its lowest elevation above the horizon. We follow [9] and [7] in assuming a minimum elevation of 5°.

## IV. SECOND ELEMENT: DEFINE A CONSEQUENCE METRIC

A consequence metric quantifies the severity of an interference hazard. Since the goal of risk analysis is to treat all hazards in equivalent ways, there should be a small number of consequence metrics (ideally just one) that characterize the severity of hazards in a uniform way.

There are many potential consequence metrics. Three broad categories are described in this section: corporate, service, and radio frequency (RF) metrics [3]. Since a judgment about the desirability of a new service requires assessing the risk of harmful interference to incumbent services, and since harmful interference is defined for regulatory purposes as a service metric of sorts, corporate or service metrics are in principle preferable to RF metrics.[1] In most cases we are aware of—such as television broadcasting, mobile public safety, and cellular service—the mapping of RF metrics to service degradation is ambiguous at best; an exception is the effect of RF interference on radar target detection [16]. Nevertheless, our analysis focuses on RF metrics since, as shown below, the available corporate and service metrics are not usable in practice.

[1] Harmful interference is defined in Article One of the ITU Radio Regulations, and incorporated into national regulations such as 47 C.F.R. 2.1 in the U.S., as ''Interference which endangers the functioning of a radionavigation service or of other safety services or seriously degrades, obstructs, or repeatedly interrupts a radiocommunication service operating in accordance with these Regulations.''

### A. CORPORATE METRICS

Corporate metrics include impacts on the ability to complete a mission (particularly for government entities); loss in revenue or loss of profit (particularly relevant to the private sector); and increased capital expenditure (relevant to both).

To the best of our knowledge, there are no publicly available corporate metrics of the ability of a MetSat service to complete the forecasting mission, even at the relatively granular level of image quality. The NOAA Office of Satellite and Product Operations maintains a web site reporting operational status for each GOES and POES satellite [17], [18], but we have been unable to find similar information for earth stations.

### B. SERVICE METRICS

Reference [9, Table 2] lists two factors that could be used as service metrics:

- the percentage of time that the link margin is not met;
- bit-error ratios (link bit-error ratio, data handling error ratio, and overall received bit-error ratio).

These metrics address availability and quality, respectively. A third factor listed in [9] is the fraction of interference-free margin consumed by interference (called $q$); this is an RF metric, discussed in Section IV.C below.

The *percentage of time that the link margin is not met* appears to determine the IPC in [9], which is a power level not to be exceeded for more than a specified percentage of time. The percentage of link outage is an attractive consequence metric in principle, since it affects received image quality. However, it is not usable in practice without a formula that relates the interference power to the percentage of link outage.

The *bit-error ratio* target in [9] appears to have been taken from SA.1025-3, and is used as a minimum performance

level. Since the bit-error ratio is a function of $E_b/N_0$, the ratio of energy per bit to noise power spectral density, it could be computed from $E_b/(N_0 + I_0)$, where $I_0$ is the interference power spectral density. However, it is not usable in practice since [9] does not provide either the formula used to relate the bit-error ratio to $E_b/N_0$, or an assumed probability distribution of $E_b$. Unfortunately, we have been unable to find any documentation on how these parameters are defined, how they are related to other tabulated parameters, or the relationship between these metrics and image quality.

Thus, neither the link margin nor the bit-error ratio metric is usable in this study.

We note that, should they become calculable, these metrics would allow harm from increased interference to be put on the same footing as harm from decreased desired signal strength. Rather merely considering interference criteria ($I$), they also include performance criteria such as the carrier to noise ratio ($C/N$). As suggested in a U.S. submission to the ITU-R [19], it is advisable to conduct interference assessments by accumulating (via dynamic simulation) the statistics of $C/(N + I)$, and to determine the complementary cumulative distribution function (CCDF) of this quantity. Bit-error ratios and link margin outage statistics can then be derived from $C/(N + I)$.

### C. RF METRICS

RF metrics are quantities observable in the radio frequency environment, such as changes in interference-to-noise ratio ($I/N$), signal to interference and/or noise ratios (SINR, $C/I$), absolute interfering signal level, receiver noise floor degradation, and so on. We discuss two candidate MetSat RF metrics: 1) the fraction of interference-free margin consumed by interference; and 2) the interfering signal power.

The *margin consumed by interference*, $q$, given in [9] is used in formulas for the permissible interference [20]:

$$I_0 = N_0 \left(M^q - 1\right) \text{ for } M > M_{min} \quad (1)$$

$$I_0 = N_0 \left(M_{min}^q - 1\right) \text{ for } M \leq M_{min} \quad (2)$$

where:

$I_0$ interference spectral density at the affected receiver (watt);

$N_0$ noise spectral density at the affected receiver (watt);

$M$ interference-free margin for the receiving system (ratio, not expressed in dB);

$q$ the fraction of the interference-free margin $M$ expressed in dB that interference may consume; [9] gives values 0.3 or 0.66 for long-term and 1.0 for short-term protection, without explanation;

$M_{min}$ the smallest interference-free margin for which the affected system must be fully protected (ratio); [9] gives a value 1.2 dB, meaning $M_{min} = 1.3$ expressed as a pure ratio, without explanation.

An interference-to-noise ratio can be derived from these equations. Inverting these formulas allows one to express $q$ as a function of $M$, $N_0$, and $I_0$:

$$q = \frac{1}{10\log(M)} \cdot 10\log\left(1 + \frac{I_0}{N_0}\right). \quad (3)$$

Thus, a Monte Carlo simulation that outputs statistics for $I_0$ could also be used to determine the likelihood of $q$ exceeding a certain value. However, the constant value of $-10$ dB in [7, Appendix 7] disregards the fact that $I/N$ is a function of the desired signal strength through the dependence on the margin $M$; either increased antenna gain or a greater antenna elevation above the horizon will improve the margin and thus $I/N$. Even though satellite communication engineers cite the amount of margin consumed by interference as a key concern, we have not found any documentation explaining the determination of acceptable $q$ values. Therefore, we do not use $q$ as a consequence metric.

A second candidate RF consequence metric, and the one that we use in this case study, is the *interfering signal power*. Reference [9, Table 1] specifies long- and short-term protection criteria, defined as the interfering signal power levels not to be exceeded more than 20% and 0.0125% of the time, respectively. We use the interfering signal power that meets the criteria in [9] to derive an exclusion distance within which LTE mobiles would not be allowed to operate (see Section V.A).

In summary, we characterize interference risk as the combination of an RF metric—specifically, the aggregate interfering signal power—and its likelihood for different hazards such as co-channel and adjacent band transmitters.

## V. THIRD ELEMENT: ASSESS LIKELIHOOD AND CONSEQUENCE

The next element of the analysis is estimating the likelihood and consequence of each of these hazards, given the parameters that affect interference (see Table 2), deployment constraints, and operating rules.

We use probability distributions for interference parameters such as the distribution of cellular mobile transmit power wherever possible, and combine them with fixed-value parameters to yield a probability distribution for the consequence metric.

The results will be quantitative versions of the qualitative likelihood-consequence chart shown in Fig. 1.

### A. MODELING METHOD

Our modeling approach builds on the method used by NTIA staff to calculate exclusion and protection zones in [6] and [7], respectively. (The protection distance is the radius of a circle around the earth station within which co-channel mobiles are not allowed to transmit without permission of the MetSat operator.)

We perform an electromagnetic compatibility analysis between cellular mobile transmitters and earth station receivers for POES transmitting in the 1695–1710 MHz band. We model interference with POES transmissions of HRPT imagery at 1707 MHz. We model a generic POES

earth station receiver based on information provided in [6, Appendix A]. Table 2 shows the parameter values we use.

We follow the assumptions of [7, Appendix 3] for mobile transmitters. We use a mobile density calculated by assuming base stations arranged in uniform hexagonal cells with inter-site distances of 1.732 and 7 km for suburban and rural deployments; this results in a base station density of 0.385 and 0.024 per sq. km for suburban and rural areas, respectively. The MetSat receiver is surrounded by suburban cells out to a 30-km distance, and rural cells beyond that.

Mobiles are randomly distributed at an average of 18 per cell, leading to a density of 6.9 and 0.42 mobiles per sq. km for suburban and rural areas, respectively.[2] We assume three 120° sectors per base station for co-band and adjacent band LTE operation. Each sector uses the same 10 MHz to serve six mobiles, each using a 1.5 MHz channel, leaving 0.5 MHz guard channels at the lower and upper ends of the bands. This results in 18 concurrently active mobiles per base station. We sample 3 and 18 mobiles per cell for the co-channel and adjacent band cases, respectively; see Sections V.B and V.C. We sample the transmit power of each mobile separately from the CDFs of EIRP given in [7].

We model path losses using the Extended Hata model. We apply it as an area model, meaning that it provides path losses for a generic terrain; it does not consider the specific terrain profile between the transmitter and the receiver [15]. This model provides the median attenuation as a function of distance between the transmitter and receiver. Table 3 provides key parameter values for the Extended Hata model.

For each mobile-MetSat link we add a location variability sampled from a zero-mean, log-normal distribution with standard deviation 8 dB (Table 4).

**TABLE 3. Extended Hata model: key parameter values.**

| Parameter | Value |
|---|---|
| Frequency | 1707 MHz |
| Clutter model | Suburban |
| Height of mobile device | 1.5 m |
| Height of base (earth) station | 20 m |
| Minimum, maximum distances | 1 km, 100 km |

The interference power levels at the MetSat receiver are calculated by aggregating the delivered signal strength from all LTE mobiles between a variable inner radius—the exclusion distance—and a fixed maximum radius. The maximum radius is chosen to be far enough beyond the exclusion distance that it includes all mobiles that contribute to the aggregate interference. The contribution of mobiles drops off with distance; in practice, we find that increasing the maximum radius more than about 10 km beyond the exclusion distance makes no difference to the received interference.

[2]We assume 10 MHz co-band and adjacent band LTE operation, with six 1.5 MHz mobile channels per 10 MHz band (mobile transmissions thus occupy 9 MHz; there are 0.5 MHz guard band at the lower and upper ends of the bands). Each cell has three sectors, for a total of 18 mobiles per band per cell.

**TABLE 4. Probability distributions used in monte carlo modeling.**

| Variable | Properties |
|---|---|
| Mobile transmit power | Distributions for suburban and rural mobiles [7, Appendix 3-3] |
| Mobile location | Randomly sampled in the plane with suburban or rural density per Table II |
| Location variability in path loss | Beyond 1 km: zero-mean log-normal distribution with 8 dB standard deviation<br>Less than 1 km: zero-mean log-normal distribution with standard deviation interpolated as a function of log distance between 0 dB at 20 m and 8 dB at 1 km |
| ACLR | Uniform distribution between 30 and 40 dB |

Since the mobiles are deployed uniformly around the earth station location and we use an area propagation model, there is no dependence on the earth station antenna pointing direction (i.e. azimuth) in this study.

We use Monte Carlo modeling for the analysis. Our algorithm is as follows:

For N iterations (we discuss the number of iterations below):

- Place mobiles randomly between the minimum and maximum simulation radius, using suburban or rural density depending on location.
- For each mobile transmitter:
  - calculate distance to the receiver;
  - calculate median path loss as a function of distance;
  - add location variability sampled from distribution;
  - sample EIRP from the distribution;
  - calculate gain given calculated angle between antenna boresight direction and vector to mobile;
  - subtract OTR and additional receiver losses;
  - calculate net interfering power for each mobile from the above, using equation (4) in Section V.B.
- For adjacent band cases:
  - subtract ACLR sampled from distribution or ACS as appropriate;
  - sum interfering power from all mobiles, using equations (5) and (6) in Section V.C.
- For co-channel cases, do the following for each exclusion distance:
  - sum interfering power from all mobiles that are at least that distance from the receiver.

Table 4 lists the probability distributions we use.

To calculate an exclusion distance, we use the long-term and short-term IPC calculated following the method in [9]. Table 5 shows the IPC for these scenarios, based on two sets of parameter values: 1) the HRPT parameters and resulting criteria given in [9, Table 2], and 2) the receiver parameters used for our case study.

Long-term and short-term interference are defined as follows:

**TABLE 5. MetSat interference protection criteria (IPC) for HRPT calculated using method in [9, Table 2].**

| | Values in [9, Table 2] | | Values used in this study | |
|---|---|---|---|---|
| Protection scenario | Long-term | Short-term | Long-term | Short-term |
| Percentage of time for link margin not met, $p$ | 0.05% | 20% | 0.05% | 20% |
| Elevation angle (exceeded for $p$) | 5° | 13° | 5° | 13° |
| Earth station antenna gain (dBic)[a] | 46.8 | 46.8 | 30.0 | 30.0 |
| Receiver reference bandwidth (kHz)[a] | 5,334 | 5,334 | 1,331 | 1,331 |
| Receiver system noise temperature (K)[a] | 320 | 210 | 320 | 210 |
| Data rate (dB-Hz)[a] | 64.2 | 64.2 | 64.2 | 64.2 |
| $q$ factor: fraction of margin (in dB) consumed by interference[a] | 0.6 | 1 | 0.6 | 1 |
| Power margin $M$ (dB) | 9.6 | 12.7 | -7.2 | -4.1 |
| Minimum margin $M_{min}$ (dB), used if power margin $M$ is negative[a] | 1.2 | 1.2 | 1.2 | 1.2 |
| $I_0/N_0$ (dB) (inferred from values in [9] using SA.1022-1) | 4.4 | 12.5 | -7.4 | -5.0 |
| Percentage of time for interference criterion | 20% | 0.0125% | 20% | 0.0125% |
| IPC (dBm) | -98 | -91 | -116 | -114 |

[a] Input values that affect calculated IPC

- *Long-term interference*: interfering signal power in the receiver reference bandwidth to be exceeded no more than 20% of the time. This scenario corresponds to a 5° antenna elevation in [9, Table 2].
- *Short-term interference*: interfering signal power in the receiver reference bandwidth to be exceeded no more than 0.0125% of the time. This scenario corresponds to a 13° antenna elevation in [9, Table 2].

Since our model assumes less earth station gain and a narrower receiver bandwidth than the example given in [9], our values are lower than the values listed there. For a 30 dBi antenna and a 1.33 MHz receiver bandwidth, the long-term IPC is 116 dBm, and the short-term IPC is 114 dBm.

We assume that the variation in transmitter location and path loss between successive Monte Carlo iterations reflects the temporal variation of interference power. Thus, we interpret the requirement in [9] that the IPC should be exceeded no more than 20% of the time as corresponding to an exclusion radius based on the 20$^{th}$ percentile of the CCDF (i.e., the exceedance probability) of aggregate interference powers.

A critical parameter to determine in Monte Carlo analysis is the number of iterations. Too few iterations give unreliable results; too many can lead to unfeasibly large computation requirements. The number of iterations needed depends on the statistics being calculated.

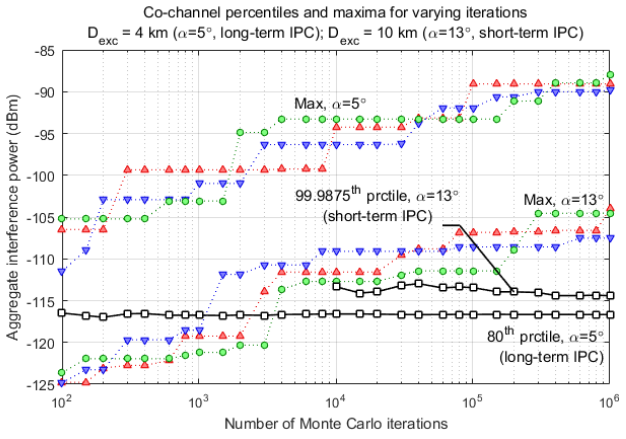


**FIGURE 4. Effect of the number of iterations on different power statistics that could be used as input to interference protection calculations: 80$^{th}$ percentile (used in long-term IPC, appropriate for elevation angle 5°), 99.875$^{th}$ percentile (used in short-term IPC, appropriate for elevation angle 13°), and maximum values taken from three independent Monte Carlo runs for elevation angles 5° and 13°.**

Fig. 4 illustrates how the calculated statistics of aggregate co-channel interference power vary with the number of Monte Carlo iterations. The results for two physical conditions are shown: antenna elevation $\alpha$ equal to 5° with exclusion distance 4 km, and antenna elevation $\alpha = 13°$ with exclusion distance 10 km. The exclusion distances selected are those needed to meet the long-term IPC (-116 dBm no more than 20% of the time) and short-term IPC ($-114$ dBm no more than 0.0125% of the time) respectively; see Section V.B for calculation details. The value 0.0125% is equal to 1/8000: if fewer than 8000 iterations are available then this percentile can only be estimated through extrapolation.

For long-term protection ($\alpha = 5°$), Fig. 4 shows the maximum and 80$^{th}$ percentile values of the calculated aggregate co-channel interference power from our Monte Carlo analysis. The maximum value is shown for three different runs of the Monte Carlo analysis (i.e., based on different sets of randomly sampled mobile locations and other characteristics).

The 80$^{th}$ percentile values changes by less than 0.2 dB as the number of Monte Carlo iterations increases from 1,000 to 10,000. We use 100,000 iterations in our analysis for long-term protection; this is a large enough number that any statistical fluctuations in the result are minimal (well under 0.1 dB).

However, the maximum value grows sharply and unpredictability with the number of iterations; it also varies dramatically from one Monte Carlo run to the next. In fact, since at least one of the distributions in the model (the location variability) is a log-normal distribution and thus has no maximum value, the value of the maximum interference power will grow arbitrarily large with a large enough number of iterations. This argues against the approach of estimating interference by taking the maximum value of a small number of iterations [7, Appendix 7].

Moving to the short-term IPC ($\alpha = 13°$), a much larger number of iterations is needed to estimate the 0.0125% exceedance value (i.e., the 99.9875$^{th}$ percentile).

We use 1,000,000 iterations in our analysis for short-term protection. The estimated 0.0125% exceedance value changes by about 1 dB between $10^5$ and $10^6$ iterations. As with the long-term case, the maximum value continues to increase as the number of iterations increases. We give more details of the statistical errors on the estimated aggregate interference power for short-term protection in Section IV.B.2 below.

### B. CO-CHANNEL TRANSMITTERS

In the co-channel case, we consider LTE operation in the same band as the MetSat receiver. As noted in Section V.A above, we posit LTE mobiles that transmit in 1.5-MHz channels; a particular mobile will hop in frequency between the six available 1.5-MHz channels in its 10 MHz block. Since we assume that all mobiles are always transmitting, there will always be one mobile transmission overlapping with the MetSat receiver bandwidth of 1.33 MHz.Thus, we sample the power of three mobiles per cell (one per sector, with six channels per sector), i.e., a density of 1.16 and 0.071 mobile per sq. km for suburban and rural areas, respectively.

We assume that the 1.33 MHz MetSat bandwidth falls completely within a 1.5 MHz LTE mobile channel. In practice, the MetSat bandwidth may fall across the boundary between two mobile channels, but since we are sampling a large number of mobiles a large number of times, this refinement will make a negligible difference.

Since not all of the transmitted power in a 1.5 MHz LTE channel is admitted into the 1.33 MHz MetSat receiver, we apply an OTR correction factor of 0.5 dB (see Section III.B.2).

In each Monte Carlo iteration, mobiles are distributed randomly between an inner and outer distance following the suburban and rural densities defined above.

#### 1) CO-CHANNEL INTERFERENCE: LONG-TERM IPC

The interference power for the $k^{th}$ mobile is calculated using the following formula, with $\alpha = 5°$:

$$P_k = T_k - OTR - L_k - L_{add} - G(\alpha, \varphi_k) \qquad (4)$$

where:

$k$-th mobile; sample 3 mobiles per base station out of total of 18;

$P_k$ interference power at the receiver input from the $k^{th}$ mobile (dBm);

$T_k$ transmitted power of the $k^{th}$ mobile (dBm);

$OTR$ on-tune rejection of 0.5 dB;

$L_k$ path loss between the $k^{th}$ mobile and the antenna input (dB);

$L_{add}$ additional losses of 1 dB;

$\varphi_k$ opening angle between antenna pointing direction and vector to $k$-th mobile;

$G(\alpha, \varphi_k)$ earth station antenna gain in the direction of the $k^{th}$ mobile, with main beam at $\alpha$ degrees elevation above the horizon (dBi).

The received interference powers of all the mobiles are converted to watts, summed, and the result converted to dBm. We calculate 100,000 aggregate interference power values.

This set of aggregate interference powers forms the basis for a quantitative risk chart. The first step is to evaluate the probability distribution for the aggregate interference at each exclusion distance. This set of distributions can be used to determine the probability that the long-term IPC of 116 dBm is exceeded for each exclusion distance.

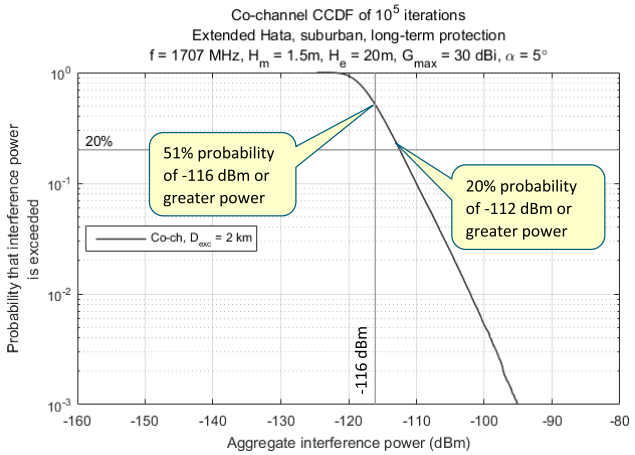


**FIGURE 5. Co-channel interference exceedance probability, short-term protection scenario (5° antenna elevation) based on an exclusion distance of 2 km.**

Consider a candidate exclusion distance of 2 km. Fig. 5 shows the exceedance probability based on all 100,000 aggregate interference powers calculated for an exclusion distance of 2 km. That is, the value on the vertical axis is the probability that the interference power on the horizontal axis is met or exceeded in the set of Monte Carlo results. The 80$^{th}$ percentile of the interference power—equivalently, as shown in this figure, the value exceeded 20% of the time—is -112 dBm. The 116 dBm long-term IPC is met or exceeded 51% of the time. Therefore, this criterion is *not* met with a 2-km exclusion distance.

Another way to investigate the co-channel interference is to plot the 80$^{th}$ percentile of the aggregate interference power as a function of exclusion distance. This is shown in Fig. 6.

The 80$^{th}$ percentile power—that is, the aggregate interference power exceeded 20% of the time—is greater than the long-term IPC of -116 dBm with an exclusion distance of 2 or 3 km, but drops below the IPC at 4 km exclusion distance. Thus, an exclusion distance of 4 km is needed to meet the long-term IPC.

Fig. 7 overlays several probability plots similar to that in Fig. 5, showing the CCDF of the aggregate interference power for multiple exclusion distances $D_{\text{exc}}$. With an exclusion distance of 4 km, the -116 dBm long-term IPC is met or

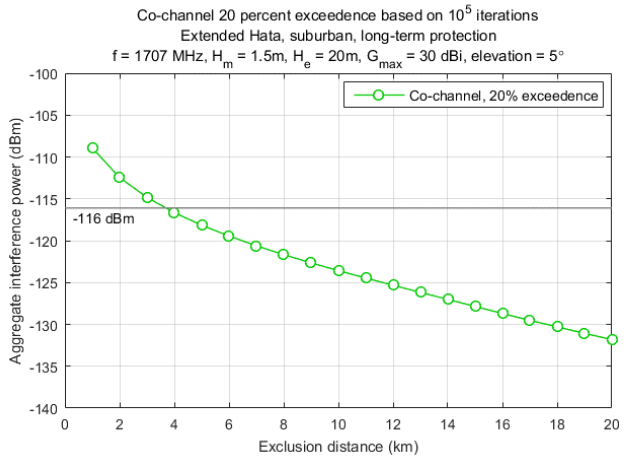


**FIGURE 6.** Co-channel interference power, 20% exceedance (i.e., 80th percentile of power) as a function of exclusion distance, long-term protection scenario (5° antenna elevation).

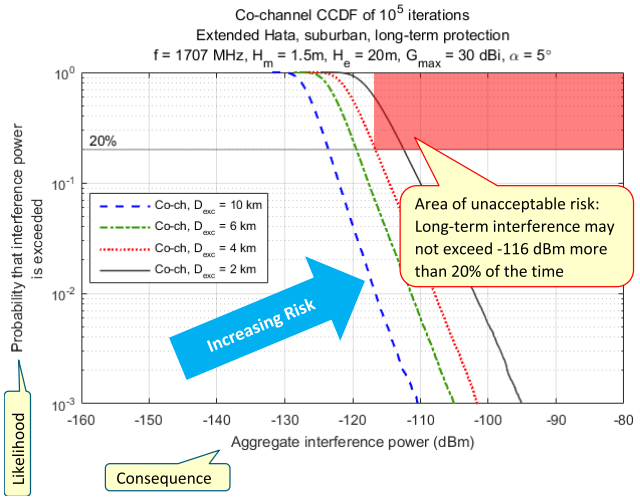


**FIGURE 7.** Co-channel interference exceedance probability, long-term protection scenario (5° antenna elevation) for various candidate exclusion distances.

exceeded only 17% of the time; therefore, this IPC is met with a 4 km (or greater) exclusion distance. Note that Fig. 7 is a risk chart (cf. Fig. 1 on p. 1), with consequence (aggregate interference power) on the horizontal axis and likelihood (probability that interference power is exceeded) on the vertical axis.

### 2) CO-CHANNEL INTERFERENCE: SHORT-TERM IPC

This section shows that, in contrast to the long-term case (5° antenna elevation), the short-term IPC (13° elevation) is not met at an exclusion distance of 4 km.

The interference power for the $k^{\text{th}}$ mobile is calculated using equation (4), as for long-term protection, except that the antenna elevation $\alpha$ is set to 13°. The received interference powers of all the mobiles are converted to watt and summed, and the result is converted to dBm. Fig. 8 shows the short-term results (13° antenna elevation) for 2, 4, 6, and 10 km

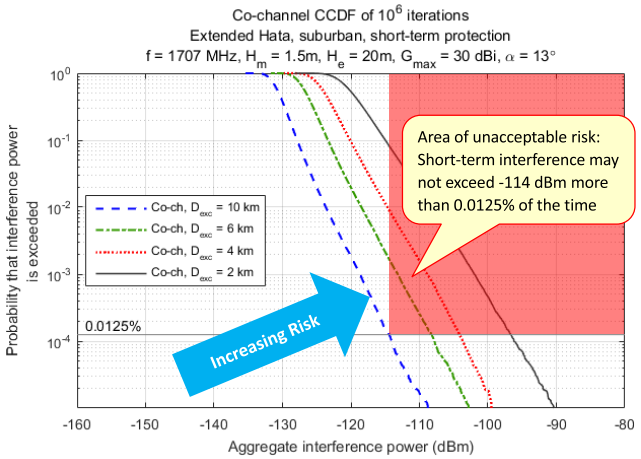


**FIGURE 8.** Co-channel interference exceedance probability, long-term protection scenario (13° antenna elevation) for various candidate exclusion distances.

exclusion distances, corresponding to the long-term results (5° elevation) in Fig. 7.

The short-term IPC is that an aggregate interference power of −114 dBm should be exceeded no more than 0.0125% of the time; this point is the lower-left hand corner of the shaded area in the chart. This short-term criterion is not met by either a 4-km or 6-km exclusion distance, but is met for a 10-km distance.

The binding constraint on co-channel interference protection is thus not interference with the earth station antenna at its lowest elevation above the horizon (the 5° long-term protection scenario) as assumed in [6] and [7], but rather the 13° elevation specified in [9] for short-term protection.

Given that this result was obtained from a Monte Carlo analysis, with statistical uncertainties as described previously, it is useful to check the level of uncertainty. Fig. 9(a) shows the same exceedance probability curves as Fig. 8, with the addition of 90% confidence intervals for each curve. The confidence intervals are calculated following Riihijärvi *et al.* [21]. Even at the extreme 0.0125% exceedance level used for the short-term IPC, the uncertainty in the aggregate interference power is small compared to the change from one exclusion distance to the next.

Fig. 9(b) is a more detailed view of the probability curve for the 10-km exclusion distance at and near the IPC, indicating the 90% confidence interval.

Fig. 9(b) also shows the equivalent probability curves calculated from four additional, statistically independent Monte Carlo calculations. At the 0.0125% exceedance probability, there is a statistical uncertainty of approximately 1 dB in the aggregate interference power.

We have not adjusted our results, e.g., by choosing the co-channel protection radius to ensure that the 90% confidence interval falls outside the IPC, since in practice the intervals can be made arbitrarily small by increasing the number of Monte Carlo iterations. More importantly, we show in the sensitivity analysis of Section VIII that there are much larger uncertainties due to other considerations.

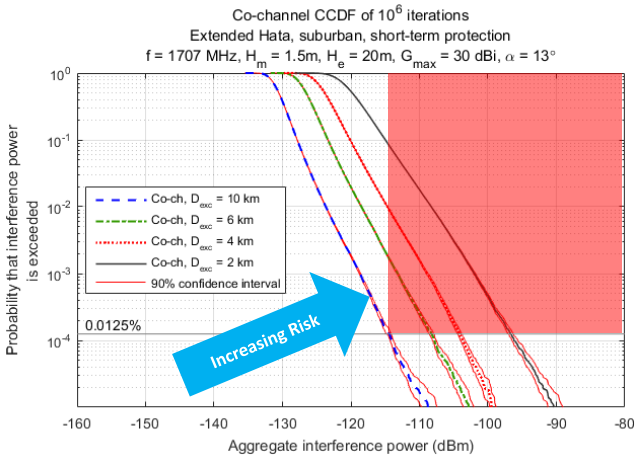


(a)

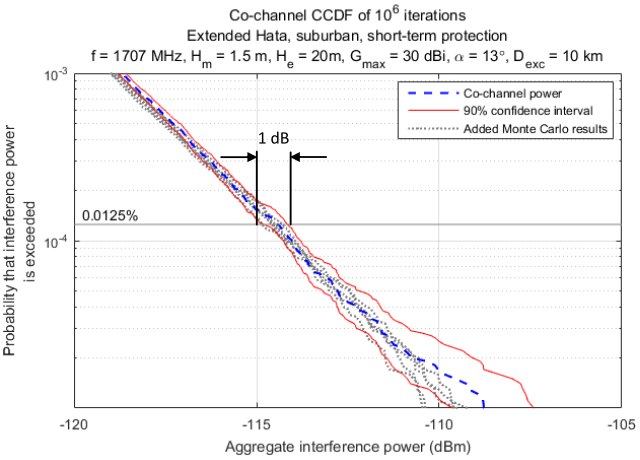


(b)

**FIGURE 9.** **Co-channel interference exceedance probability, short-term protection scenario (13° antenna elevation) for various candidate exclusion distances; 90% confidence limit shown for each exceedance probability. (a) Full probability chart. (b) Detailed view of previous chart for the 10-km exclusion distance, showing 1 dB uncertainty in the aggregate interference power.**

### C. ADJACENT BAND TRANSMITTERS

Cellular mobiles have been operating in the adjacent AWS-1 A block (1710–1720 MHz) for some years, close to the three POES center frequencies of 1698, 1702.5 and 1707 MHz.

We model interference from the adjacent band to the MetSat service at the operating frequency closest to the band edge, 1707 MHz. We assume that the adjacent channel LTE transmissions have the same characteristics as those assumed for the co-channel interferer, e.g., the same base station density, distribution of mobile transmit power, and body loss.

Although AWS-1 mobile transmitters in the adjacent band can be at an arbitrarily short distance from a MetSat receiver, for practical and modeling purposes we assume a 20-meter exclusion zone for transmitters in the adjacent 1720–1720 MHz block. This distance is typically inside the perimeter of a MetSat site. Since the Extended Hata model only applies for distances greater than 1 km, we interpolate between the free space path loss at 20 meters and the Extended Hata value at 1 km. We likewise interpolate the standard deviation of the location variability between 0 dB at 20 m and 8 dB at 1 km.

We consider two interference hazards linked to the adjacent band: OOBE and ABI. Unlike the co-channel case where we only sample the power of the one in six mobiles in a 10 MHz block whose transmission overlaps the MetSat receiver channel, in this case we sample the power of all six mobiles in every 10 MHz sector because they all leak power into the MetSat channel.

#### 1) OUT-OF-BAND EMISSION

The 3GPP specification for mobile ACLR is 30 dB anywhere outside the operating band. In practice, mobile ACLR performance exceeds the minimum required by the standard, although it varies from device to device; see e.g. Ofcom [22, Fig. 5]. In the absence of data for AWS-1 devices, we assume that ACLR is sampled from a uniform distribution between 30 and 40 dB. (Variations are explored in Section VIII.D.)

We assume that any of the mobiles in the adjacent 10 MHz A-block will deliver power reduced by the sampled ACLR in the MetSat receiver channel. As explained in Section V.A above, we assume 18 active mobiles per base station in a 10 MHz block.

Just as in the co-channel case, we test for both the long- and short-term interference scenarios defined in [9].

The interference power for the $k^{\text{th}}$ mobile in the long- and short-term scenarios is calculated using the following formula, with the antenna elevation $\alpha$ set to 13° and 5° respectively:

$$P_k = T_k - ACLR_k - OTR - L_k - L_{add} - G(\alpha, \varphi_k) \quad (5)$$

where $ACLR_k$ is the adjacent channel leakage ratio of the $k^{\text{th}}$ mobile, from a uniform [30, 40] dB distribution, and the other variables are as given above.

**TABLE 6.** **ACS mask for Elmendorf AFB.**

| Frequency offset | Attenuation |
|---|---|
| ± 0.665 MHz | -3 dB |
| ± 1.34 MHz | -20 dB |
| ± 12 MHz | -60 dB |

#### 2) ADJACENT BAND INTERFERENCE

We model the interference from energy in the adjacent channel that is not rejected by the MetSat receiver by using the ACS mask for Elmendorf AFB shown in Table 6 [6, Appendix A, Table A22].

This mask is the least selective of the typical patterns reported by the NTIA. We investigate the more selective mask

given for the Fairbanks Command and Data Acquisition Station (FCDAS) site in the sensitivity analysis, Section VIII.C.

We assume that the mask is linear in the dB scale. Since the transmit power of mobiles in each of the six 1.5 MHz channels in the adjacent 10 MHz block is constant over its channel, we convert the ACS mask to the linear scale, average the attenuation over each 1.5 MHz channel, and then convert back to dB. This results in the following ACS values for the six channels: {30.6, 36.2, 41.9, 47.5, 53.1, and 58.6 dB}, shown in Fig. 10.

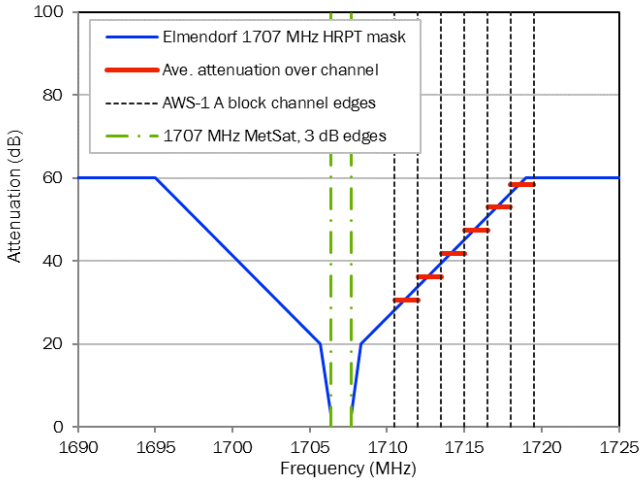


**FIGURE 10.** MetSat adjacent channel selectivity.

As before, we test for both the long- and short-term interference scenarios. The interference power for the $k^{\text{th}}$ mobile in the long- and short-term scenarios is calculated as follows:

$$P_k = T_k - ACS_k - OTR - L_k - G(\theta, \varphi_k) \qquad (6)$$

where $ACS_k$ is the adjacent channel selectivity of the $k^{\text{th}}$ mobile, taken from {30.6, 36.2, 41.9, 47.5, 53.1, 58.6} dB, and the other variables are as given above.

### 3) RESULTS

The results for OOBE and ABI in both the long-term (5° elevation, 20% of time) and short-term (13° elevation, 0.0125% of time) interference scenarios are shown in Fig. 11.

OOBE and ABI pose a similar risk level, although the risk from ABI is somewhat lower than OOBE. The risk for OOBE may be slightly higher than calculated, since we do not model interference from AWS-1 mobiles in the rest of the band, i.e. blocks B to F. However, since ACLR drops off with distance from the passband ([22, Fig. 5]), this increased risk is likely to be small.

The curves for the long- and short-term scenarios are very close to each other. The elevation angle makes little difference to the aggregate interference power because the mobiles that contribute most to the aggregate power are very close to the antenna, and are therefore at a large angle below the antenna boresight. Thus, they are outside the main beam whether the antenna elevation angle is 5° or 13°. Once they are in the side

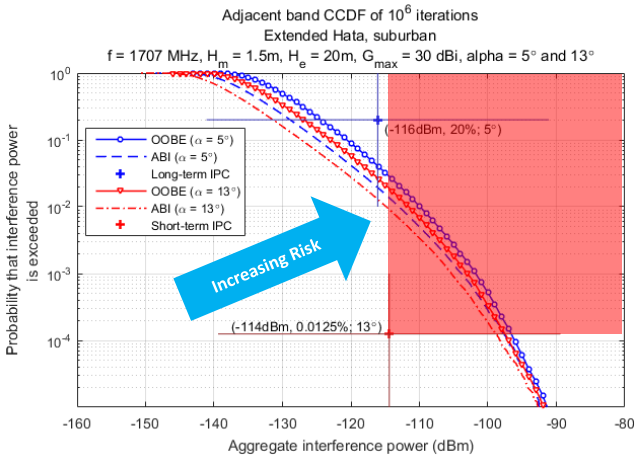


**FIGURE 11.** Interference from adjacent band transmitters.

lobes, the distance from the main beam becomes irrelevant—the gain pattern is flat.

Fig. 11 shows that interference from mobiles in the adjacent AWS-1 band violates the (13°, 0.0125% of time) short-term IPC of 114 dBm, though not the long-term IPC. The AWS-1 band was auctioned in 2006, and is in use in most locations. The modeling results imply significant interference to MetSat operation from current AWS-1 services, but none has been reported to our knowledge. One or more of the following reasons may account for this:

- The long- and short-term IPC specified in [9] are unnecessarily conservative; in other words, interference at levels greater than these limits is not, in fact, harmful.
- Other parameter values in our model (see Table 2; similar values were used in [6] and [7]) are too conservative, overestimating the resulting mobile interference power or underestimating the MetSat receiver's robustness.
- The path loss model we use does not provide enough attenuation, leading to an overestimate of the aggregate interference power.
- The current model assumes a 20-m exclusion zone for AWS-1 mobiles; perhaps it should be greater.

We compare adjacent band to co-channel interference in the next section.

## VI. FOURTH ELEMENT: AGGREGATE LIKELIHOOD-CONSEQUENCE RESULTS

Once likelihood-consequence data have been collected for the relevant hazards, they can be plotted on a risk chart to present an aggregate view.

As noted in [1, Sec. 3.C], risk charts can be used in several ways to support regulatory decisions. Fig. 7 and Fig. 8 are of one type, showing the likelihood-consequence curves for different potential choices of operating parameters. In this section, we give another type of risk chart: we compare the risk of different interference modes, specifically the relative risk of interference from co-channel and adjacent band trans-

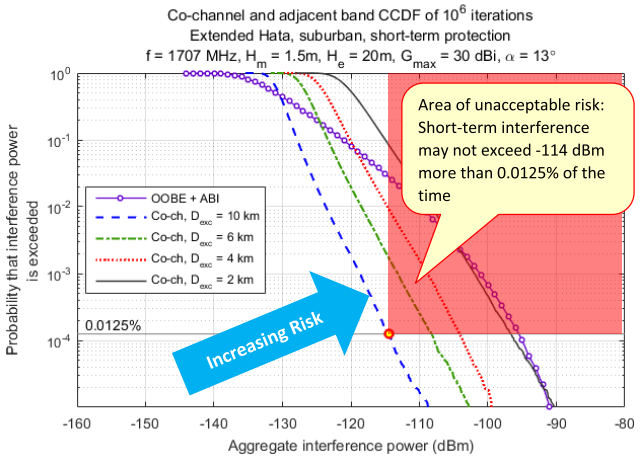


**FIGURE 12.** **Aggregated results: Interference exceedance probability for short-term protection various co-channel exclusions, and 20 m adjacent band exclusion.**

mitters, on the same chart. Since OOBE and ABI are of a similar magnitude, we sum them and show the risk from adjacent band transmitters as a single line.

As seen above, the (13°, 0.0125%) short-term criterion is the binding co-channel constraint. Fig. 12 shows that a 10-km exclusion distance provides protection against short-term co-channel interference. However, the interference from adjacent band transmitters is evidently much higher—it is similar to that from co-channel interferers based on a 2-km exclusion distance.

Let us assume that the interference level generated from the adjacent band is an acceptable benchmark (given the absence of any concern by MetSat operators about this source, which has been active for many years now). If the aim is simply to equalize co-channel and adjacent band interference, Fig. 12 shows that a 2km co-channel exclusion distance is acceptable.

To summarize our findings:

- Protecting the 5° antenna elevation scenario (as was done in [6] and [7]) yields an exclusion distance of 4 km for the long-term IPC defined in [9]; see Fig. 7.
- An exclusion distance of 4 km is not good enough for (13°, 0.0125% time) short-term protection, though. For that one needs 10 km; see Fig. 8.
- The interference from adjacent band transmitters is much higher than from co-channel ones. If the aim is to equalize co-channel and adjacent band interference, then a 2-km exclusion distance suffices; see Fig. 12.

Since no interference has been reported from the already-operating adjacent AWS-1 band (for example, the topic did not come up in any of the CSMAC WG-1 discussions, according to participants), we believe that either the IPC in [9] and/or other NTIA modeling assumptions in [6] and [7] that we have adopted are too conservative.

While our results are not directly comparable with those in [7] (see Section II.A above), some observations are in order. None of the NTIA protection distances for POES are less than 20 km, and they are more than 50 km on average [7, Table 7 in Appendix 7]. Our results suggest that the protection zones adopted by the FCC are extremely conservative.

## VII. FURTHER ASPECTS OF AN INTERFERENCE ANALYSIS

The four elements of the risk-informed interference assessment described in Sections II to VI does not provide a complete coexistence analysis. We briefly discuss other perspectives that should be considered.

### A. BASELINE SYSTEM PERFORMANCE

The risk of interference to a system can only be accurately assessed in the context of the baseline performance in the absence of added interference from a new service, i.e., in the context of pre-existing risks.

Anecdotal evidence in [3] suggests that of the order of 10% of MetSat images received at Juneau, AK show significant degradation. This indicates that there are non-trivial baseline harms in the absence of the new service interference modeled in this study, due perhaps to variations in satellite signal quality due to ionospheric scintillation, non-RF effects such as satellite tracking error or component failure, and/or existing cellular operation in the adjacent AWS-1 band.

### B. MITIGATION

Any assessment of interference risk makes assumptions about the design and operation of interfering transmitters and affected receivers. Harm may be mitigated by changes in system parameters, for example by changes in equipment or deployment.

In the MetSat case, for example, we assume that the earth station receiver will absorb all interference arriving at its location. However, clutter fencing can significantly reduce the interference impinging on the antenna, especially for sensitive configurations such as the 5° and 13° elevation conditions modeled above.

Mitigation can also occur at the transmitters. For example, within a specified mitigation distance, LTE mobiles could refrain from transmitting on channels that overlap a MetSat channel in use during a satellite transit; in this case, the risk assessment would include consideration of adjacent channel interference, but not co-channel interference, from mobiles in the MetSat band. Another possibility would be to reduce the maximum transmit power of mobiles within the mitigation distance.

A mitigation that would obviate the co-channel risk analysis completely would be to shut down LTE operation during the few short time periods every day when satellites are rising and at their most susceptible. At worst, LTE operation could be shut down during the handful of 10 minute daily transits from three NOAA POES and two EUMETSAT Metop spacecraft, the operational set at the time of writing [18].

Once a mitigation is proposed, the analysis would begin anew to take it into account.

### C. COST-BENEFIT ANALYSIS

A risk assessment establishes the likelihood and consequence of hazards such as those caused by adjacent band transmission with a given set of service rules. Any set of service rules will impose costs on the affected system and accrue benefits to the transmitter; the costs and benefits will differ from one rule set to another. Risk assessment provides a well-reasoned engineering basis for the scenarios for which costs and benefits are calculated, but does not address the economic trade-offs.

### D. PEER REVIEW

Independent review of risk assessment studies is a common best practice [23]. We have tried to facilitate review of this work by publishing the source code of the simulation model and making our spreadsheet calculations available.[3] We look forward to feedback from the community.

## VIII. SENSITIVITY ANALYSIS

### A. OVERVIEW AND SUMMARY

The model presented here involves many interacting parameters. A sensitivity analysis explores which parameters have a particularly strong influence on the outcome. In a specific case, this can inform the judgment that the regulator must make about whether the calculated risks are a sufficiently accurate basis for rulemaking; it can also lead to insights about which mitigation strategies to pursue.

We perform a sensitivity analysis that investigates the effects of three general classes of parameters on the predicted interference power, and thus the exclusion distance:

- propagation modeling (Extended Hata vs. ITM, urban and suburban clutter, ITM terrain characterization, and location variability in Extended Hata);
- earth station characteristics (antenna gain, antenna elevation angle, antenna height, and the system's ACS);
- out of band emitter characteristics (out of band emitter frequencies, OOBE filtering for existing mobiles).

Table 7 lists the baseline values of these parameters (i.e., the values used in our case study). The hazard criterion we use is the short-term IPC (13° elevation): for a 30 dBi antenna gain, the aggregate interference power may not exceed -114 dBm more than 0.0125% of the time. As shown above, this condition reflects the greatest co-channel interference hazard.

We explore the different parameters in Sections VIII.B to VIII.D below, and provide graphic illustrations of the results in Section VIII.E.

Table 8 summarizes the results for all cases in the sensitivity analysis. This table clearly shows that the most significant uncertainty is associated with the propagation modeling—the selection of propagation model, the clutter model, and the location variability. These elements are discussed further in Section VIII.B. Changes in the propagation and clutter models can change the aggregate interference power by more than 20 dB, and can increase the exclusion distance from about 10 km to more than 60 km. The effects of the different elements of propagation modeling are as follows:

- *Selection of model type (Extended Hata or ITM)*. For like-to-like comparisons (e.g. Extended Hata and ITM, both with suburban clutter, and with average terrain $\Delta h = 90$ m in ITM), the differences in path loss are less than 5 dB.
- *Clutter model*. This is the most critical aspect of propagation modeling; the path loss changes by tens of dB depending on whether rural, suburban, or urban conditions are selected.
- *Standard deviation of location variability*. For the short-term IPC, increasing the standard deviation of location variability by 2 dB leads to an increase of 6 to 8 dB in the aggregate interference power.
- *Terrain roughness $\Delta h$ in ITM*. Moving from 90 m to 30 m decreases the path loss by 5 to 10 dB.

Moving to the earth station characteristics: major changes such as increasing the antenna height from 20 m to 55 m can change the aggregate interference power by up to 10 dB; see Section VIII.C. However, these changes reflect knowable variability from one station to the next—not modeling uncertainty. Less major changes, such as an increase in the antenna height from 20 m to 35 m or in the antenna gain, typically modify the calculated aggregate interference power by no more than 6 dB.

Changes in the characteristics of out of band emitters change the aggregate interference by smaller amounts; see Section VIII.D.

The sensitivity analysis does not change the basic conclusions that the short-term IPC is the binding constraint, and that adjacent channel interference is much higher than co-channel interference given a co-channel exclusion distance based on the IPC. The 2-km exclusion distance that suffices in the baseline case if the aim is to equalize co-channel and

**TABLE 7. Baseline parameters for sensitivity analysis.**

| Parameter | Value |
|---|---|
| *Propagation Modeling* | |
| Model family | Extended Hata |
| Clutter type | Suburban |
| Location variability | Normally distributed in dB, standard deviation 8 dB |
| *Earth Station Characteristics* | |
| Maximum antenna gain | 30 dBi |
| Antenna elevation angle | 13 degrees |
| Antenna height | 20 meters |
| ACS | Less selective option, based on Elmendorf AFB (see Fig. 10) |
| *Out of Band Emitter Characteristics* | |
| OOBE frequencies included | A block only (10 MHz bandwidth, first adjacent AWS 1 block) |
| OOBE filtering | Uniformly distributed, 30 to 40 dB |

[3]The spreadsheet showing IPC calculations is at http://bit.ly/Calculator-SA1026-4, and the MATLAB scripts for interference calculations are at http://bit.ly/Scripts-MetSat-RIA.

**TABLE 8. Summary of results for sensitivity analysis.**

| | Co-channel exclusion distance (km)[a] | | Interference power, dBm, short-term protection; co-channel based on 10 km exclusion distance[a] | | |
|---|---|---|---|---|---|
| Parameter / Value | From IPC | Match OOBE+ABI | OOBE | ABI | Co-channel |
| *Baseline analysis* | *10* | *2* | *-97* | *-98* | *-114* |
| | Co-channel exclusion distance (km)[a] | | Change in interference power, dB, short-term protection; co-channel based on 10 km exclusion distance[a] | | |
| Parameter / Value | From IPC | Match OOBE+ABI | OOBE | ABI | Co-channel |
| *Propagation model and clutter (baseline: Extended Hata, suburban)* | | | | | |
| Extended Hata, urban | 5 | <1 | -1.4 | -1.6 | -9.2 |
| ITM, Δh = 10 m, rural, base ITM case | 60 | 10 | 4.6 | 4.8 | 23 |
| ITM, Δh = 30 m, rural, base ITM case | 67 | 11 | 3.8 | 3.9 | 23 |
| ITM, Δh = 30 m, suburban, 15 dB correction | 39 | 8 | 1.0 | 1.0 | 17 |
| ITM, Δh = 30 m, urban, 27 dB correction | 18 | 3 | -1.1 | -1.1 | 7.3 |
| ITM, Δh = 90 m rural, base ITM case | 65 | 11 | 1.7 | 1.9 | 21 |
| ITM, Δh = 90 m, suburban, 15 dB correction | 27 | 5 | -0.7 | -0.9 | 12 |
| ITM, Δh = 90 m, urban, 27 dB correction | 11 | <1 | -2.4 | -2.6 | 0.6 |
| *Location variability (baseline: 8 dB)* | | | | | |
| 6 dB | 6 | 2 | -0.3 | -0.2 | -7.1 |
| 10 dB | 18 | 4 | 0.4 | 0.2 | 7.4 |
| 12 dB | 29 | 7 | 1.3 | 1.2 | 15 |
| *Antenna height (baseline: 20 meters)* | | | | | |
| 15 meters | 8 | 2 | 1.3 | 1.0 | -4.3 |
| 35 meters | 16 | 4 | -3.0 | -2.6 | 5.1 |
| 55 meters | 22 | 7 | -5.1 | -4.8 | 9.1 |
| *Antenna gain / short-term protection limit (baseline: 30 dBi / -114 dBm)* | | | | | |
| 40 dBi / -105 dBm | 4 | 2 | -2.5 | -2.5 | -2.5 |
| *Antenna elevation (baseline: 13 degrees)* | | | | | |
| 20 degrees | 8 | 2 | -0.1 | -0.5 | -3.6 |
| *ACS (baseline: from Elmendorf AFB; wider frequency mask)* | | | | | |
| From FCDAS; narrower frequency mask | - | - | - | -10.3 | - |
| *OOBE frequencies (baseline: A block, 10 MHz)* | | | | | |
| A and B blocks, 20 MHz total | - | - | 1.6 | - | - |
| *OOBE filtering (baseline: ACLR is uniformly distributed, 30 to 40 dB)* | | | | | |
| Fixed at 30 dB | - | - | 3.8 | - | - |
| Fixed at 40 dB | - | - | -6.2 | - | - |

[a] See Section VIII.E for a graphic illustration of these values

adjacent band interference can grow, as shown in Table 8, but not dramatically. For example, ITM with $\Delta h = 90$ m and suburban clutter yields a 5-km exclusion distance.

### B. PROPAGATION MODELING

As shown above, changes in propagation modeling can change the predicted path losses by tens of dB. It would therefore be no surprise if the resulting exclusion distances depended strongly on the choice of propagation model. We find that the exclusion distance can vary from 5 km to more than 60 km depending on the propagation model and—critically—on assumptions regarding clutter (rural, suburban, or urban); see Table 8. However, we find that different models give more similar results if assumptions are matched: e.g., exclusion distances with suburban clutter and typical terrain are 10 km and 27 km for Extended Hata and ITM, respectively.

#### 1) EXTENDED HATA MODEL AND ITM

In our sensitivity analysis, we compare the Extended Hata model (used in our baseline analysis) and ITM [24] (used in [6] and [7]).

The Extended Hata model is an empirical model of radio propagation. It is based on an extensive data set measured by Okumura *et al.* [25], throughout Japan but primarily in Tokyo. Hata [26] developed empirical formulae that fit nomographs prepared by Okumura for flat terrain (terrain height variations of 20 m or less); distances 1 to 20 km; frequencies 150 to 1,500 MHz; and for urban and suburban conditions. Reference [15] extended Hata's formulae to cover distances

**TABLE 9. ITM parameters used in sensitivity analysis.**

| Parameter | Value(s) | Comment |
|---|---|---|
| Prediction mode | Area prediction mode | Appropriate for general analysis (e.g., [6]). The point-to-point mode, which calculates path loss based on a specific terrain profile, is appropriate for decision-making at a specific site (e.g., [7]). |
| Terrain roughness, $\Delta$h | 10 m, 30 m, 90 m | 10 m and 30 m are used in [6], while 90 m is recommended as a default value in [24]. |
| Mode of variability | Mobile mode | Appropriate for the situation where a fixed earth station is subject to interference by mobile transmitters [31]. |
| Confidence level | 50% | This value provides information about the interference experienced by a typical earth station [31]. |
| Location variability | Approximately normally distributed in dB, mean 0 dB, standard deviation varies | Standard deviation calculated from ITM results; increases with increasing $\Delta$h and with range. Values vary from 6 to 10 dB at range 1 km to 13 dB at 100 km [31]. |
| Antenna heights | 20 m (earth station)<br>1.5 m (mobiles) | Matches the baseline analysis. |
| Frequency | 1707 MHz | Matches the baseline analysis. |
| Siting | Careful (earth station)<br>Random (mobiles) | The earth station is unlikely to be placed at a particularly low elevation. However, its location is also not optimized for terrestrial coverage. Therefore, careful placement seems appropriate. |
| Urban clutter | Urban: 27 dB<br>Suburban: 15 dB<br>Rural: 0 dB (base ITM calculation) | Based on Okumura *et al.* [25]. 27 dB is less than the correction for urban clutter given by Longley [30]; see [31]. |
| Other parameters | ITM default values | Model results are generally insensitive to other ITM parameters at 1707 MHz. |

up to 100 km and frequencies 1,500 to 3,000 MHz. We use the Extended Hata model of [15] with suburban clutter for our baseline analysis; the sensitivity analysis also considers urban clutter.

ITM is based on the Longley-Rice model of radio propagation [27]. This model is based on radio propagation theory, using measurements in the US and worldwide for calibration. The Longley-Rice model was tested and developed further through measurement programs in rural areas of the U.S. [28], [29]. ITM often gives much lower path losses and much larger exclusion distances than Extended Hata. However, it has been known for decades that ITM significantly underestimates attenuation (by tens of dB) in urban areas and that a correction for urban clutter is needed [30, Table 2].

ITM can be run in *area mode*—where terrain height variations are described through a single terrain roughness parameter $\Delta$h—and *point-to-point* mode, where a digital terrain model (DTM) provides the terrain elevation along a path between the transmitter and the receiver. This study considers a generic location, which means that area mode is appropriate.

Table 9 lists the ITM parameters that we use in the sensitivity analysis. More details of ITM, including the rationale for our parameter selection, are given in [31].

#### 2) URBAN, SUBURBAN, AND RURAL CONDITIONS

The Extended Hata propagation model used in our baseline analysis is based on measurements reported in [25]. These measurements focused on urban conditions, with corrections for suburban, rural, and open areas. In contrast, as just stated, ITM is most appropriate for use in rural areas.

We investigate the effects of applying a correction factor to ITM to account for suburban or urban clutter. Following Longley [30], we base these correction factors on Okumura's measurements [25], [31]; Table 9 shows the values we selected. We also investigate the urban version of the Extended Hata model [15].

#### 3) RESULTING PATH LOSS

Fig. 13(a) shows the calculated path loss as a function of range for the Extended Hata model with suburban clutter (the baseline analysis) and for ITM with no clutter correction (i.e., under rural conditions) with three different values of the ITM terrain roughness parameter $\Delta$h. The terrain roughness $\Delta$h is defined as the difference between the $90^{\text{th}}$ and the $10^{\text{th}}$ percentile of the terrain elevation. For average (relatively hilly) terrain, [24, Table 2] recommends $\Delta h = 90$ m; flat plains have $\Delta h = 30$ m. In the continental U.S., $\Delta$h falls below 10 m only at the mouth of the Mississippi, the tip of Florida, and a narrow strip of the East Coast [24, Fig. 3].

The uncorrected ITM path losses are much lower than the Extended Hata losses, which means that ITM would predict much greater interference. However, an uncorrected ITM is inappropriate for modeling urban and suburban settings for any value of $\Delta$h.

Fig. 13(b) shows path loss as a function of range, focusing on the effect of urban and suburban clutter. For clarity, ITM results are only shown for $\Delta h = 90$ m.

Table 10 summarizes the full set of path losses at 10 km range. For like-to-like comparisons (e.g. Extended Hata, and ITM with the equivalent clutter model and typical terrain roughness $\Delta h = 90$ m) the differences are of the order of 5 dB. The effect of adding suburban or urban clutter to

**TABLE 10. Path loss for different models and conditions at 10 km range.**

| Model | Δh | Path loss at 10 km (dB) | | |
|---|---|---|---|---|
| | | Urban | Suburban | Rural |
| Extended Hata | N/A | 170 | 161 | N/A |
| ITM | 90 m | 168 | 156 | 141 |
| ITM | 30 m | 160 | 148 | 133 |
| ITM | 10 m | 158 | 147 | 132 |

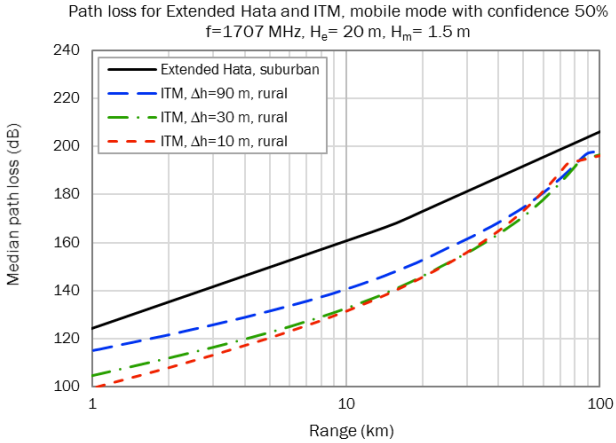


**FIGURE 13. Path loss as a function of range for Extended Hata and ITM. (a) Extended Hata with suburban clutter vs. ITM with no clutter correction (rural case) with ITM Δh = 90 m, 30 m, and 10 m. (b) Extended Hata with urban and suburban clutter vs. ITM Δh = 90 m with urban, suburban, and rural clutter.**

ITM is much greater than the effect of varying Δh, or of selecting the Extended Hata model.

#### 4) LOCATION VARIABILITY

We use the phrase *location variability* to describe random fluctuations in the path loss. Our baseline analysis describes the location variability using a normal distribution (in dB) with mean 0 dB and standard deviation 8 dB. In the sensitivity analysis, we consider values between 6 and 12 dB for the standard deviation of location variability with Extended Hata. The analysis shows that an increase of 2 dB in location

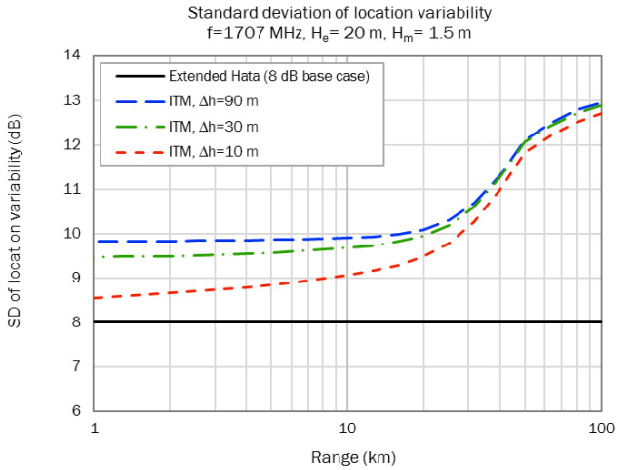


**FIGURE 14. Standard deviation of location variability for ITM and Extended Hata.**

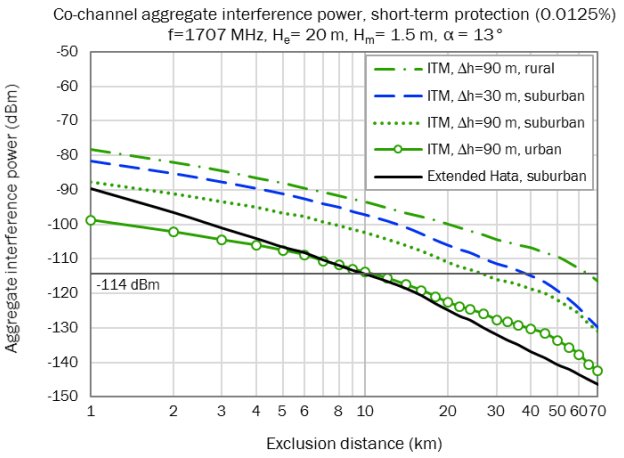


**FIGURE 15. Aggregate interference power as a function of exclusion distance for five different propagation cases: other propagation cases are not shown for clarity.**

variability leads to an increase in short-term aggregate interference power of 6 to 8 dB.

When using ITM, we use a range-dependent standard deviation, as described in [31]. ITM calculates a location variability that is approximately normally distributed in dB. Fig. 14 shows the standard deviation we used with ITM, together with the baseline 8 dB.

#### 5) DISCUSSION

Changing the propagation model from Extended Hata suburban to ITM with no clutter correction (i.e., rural) decreases the path loss by more than 20 dB. However, this is an inappropriate comparison because it does not compare like environments.

Fig. 15 shows the short-term co-channel aggregate interference power as a function of exclusion distance. It compares the baseline case (Extended Hata, suburban) and four of the ITM cases (not all ITM cases are shown for clarity). The difference in path loss leads to a difference

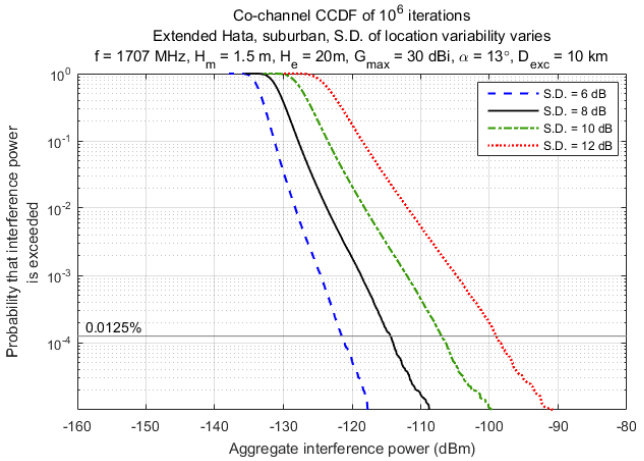


**FIGURE 16.** **Co-channel interference exceedance probability, short-term protection scenario, based on the Extended Hata suburban model with different values for the standard deviation of the location variability.**

in the aggregate interference power, which in turn can lead to huge increases in the exclusion distances—up to more than 60 km if the base (rural) version of ITM is used. This highlights the importance of using an appropriate clutter model in interference analyses.

Fig. 16 shows the co-channel interference power for values of the standard deviation of location variability between 6 dB and 12 dB. As the exceedance probability decreases, the curves move farther apart. For an exceedance probability of 20% (long-term protection), the curves are about 4 dB apart: an increase of 2 dB in the standard deviation of location variability gives an increase of 4 dB in aggregate interference power. However, at 0.0125%, the curves are 6 to 8 dB apart. These relatively extreme interference cases are associated with path losses that lie three to four standard deviations below the median loss. This highlights that the statistics of path loss, as well as the median value, must be considered in any interference analysis.

#### 6) PRESENT-DAY SUBURBAN AND URBAN CONDITIONS

We believe that propagation in present-day suburbs should be modeled as urban, not suburban, in terms of the Okumura-Hata model family. Okumura's measurements were performed in 1963 and 1965 in Japan. The "urban" transects were taken from Tokyo, which might sound stereotypically urban. However, the first skyscraper in Japan was not completed until 1968; Japanese building codes prohibited buildings higher than 31 m until 1963 [32]. Therefore, the Tokyo of Okumura's measurements was free of the high buildings typical of present-day big cities.

Fig. 17 compares aerial views of 1960s Tokyo; present-day Seattle; and present-day Kirkland, a suburban satellite of Seattle. Outlying portions of Tokyo were less built up, as are the outlying portions of Seattle and Kirkland today.[4]

[4]Kirkland was selected for this comparison simply because two of the authors live there. This selection avoided any temptation to "cherry-pick" the suburban area that looks best for our case.

The buildings in 1960 Tokyo are clearly larger than those in Kirkland. However, the comparison between 1960 Tokyo and present-day Kirkland is much closer than that between 1960 Tokyo and present-day Seattle—the buildings in Seattle are up to 10 times taller.

Therefore, "urban" clutter as measured by [25] and as defined in the Extended Hata model is likely to represent propagation in present-day suburbia—not in big cities.

### C. EARTH STATION CHARACTERISTICS

We consider variations in the earth station design: the height and gain of the earth station antenna; its elevation angle; and the ACS. While these are fixed and known for a given location, the analysis gives an indication of how sensitive the results are to errors in the assumed parameter values.

Table 11 lists the characteristics of three earth stations analyzed in [6] and [7], together with the characteristics used in our case study. The earth station for our case study has similar characteristics to the earth station at Elmendorf AFB, except that the antenna height is lower.

Our sensitivity analysis includes parameter values that cover the bulk of conditions shown in the earlier studies.

*Earth station antenna height.* Intuitively, a higher antenna would receive more interference from mobiles because of lower path losses, although this would be slightly offset by differences in the earth station antenna gain to the mobile locations. Reference [6] shows that 33 m is a common height (all the military sites are shown as 33 m). The lowest antenna height is 14.5 m. The highest antenna, at Suitland, is given as 86.8 m.

Our base condition uses a 20-m antenna height; we investigate values of 15 m, 35 m, and 55 m here.

*Earth station antenna gain.* We assume 30 dBi for the earth station antenna main beam gain. Increased gain would decrease the susceptibility to interference, since the gain in the horizontal direction (typically 5° below the antenna elevation angle) would be lower. A higher antenna gain would also increase the strength of the desired satellite signal, leading to a higher IPC value. 30 dBi is a common value for the gain: [6] gives a gain between 29 and 31 dBi for most sites. The highest gain reported in [6] (for two sites) is 43.1 dBi; we investigate 40 dBi in the sensitivity analysis. The corresponding short-term IPC increases from 114 dBm at 30 dBi to 105 dBm at 40 dBi.

*Earth station antenna elevation angle.* The baseline analysis assumes 5° antenna elevation for long-term protection and 13° for short-term protection, matching the IPC in [9]. Higher antenna elevation angles would decrease the susceptibility to interference as long as the horizontal direction remains within the main lobe of the antenna gain. However, once the antenna elevation is high enough that all interfering transmitters lie in the side lobes, further increases in antenna elevation have little further effect on the interference power. (Our model of the antenna gain is simplified, such that individual side lobes are not modeled—outside the main lobe, the antenna gain reaches a plateau). In our sensitivity analysis, we investigate

**FIGURE 17.** Views of 1960s Tokyo, and present-day Seattle and Kirkland, WA. (a) Tokyo, approx. 1960: Yurakucho. Maximum building height 31 m (102 ft.). (b) Tokyo, approx. 1960: Shibuya. Maximum building height 31 m (102 ft.). (c) Downtown Seattle, WA, present day. Maximum building height 287 m (943 ft.); 150 m (500 ft.) is common. (d) Downtown Kirkland, WA, present day. Maximum building height 17 m (55 ft.). Photograph source: Wikimedia Commons.

**TABLE 11.** Earth station characteristics for illustrative cases in [6], [7] and for our base condition.

| Parameter | Sioux Falls (Table A-7) [a] | Elmendorf AFB (Table A-22) | Monterey, CA (Table A-24) | Current document, baseline analysis |
|---|---|---|---|---|
| Antenna height (m) | 14.5 | 33 | 33 | 20 |
| Main beam gain (dBi) | 31 | 29 | 29 | 30 |
| ACS: frequency difference at -60 dB point (MHz) | 6.64 | 12 | 12 | 12 |
| Terrain type [b] | 15 km from the outskirts of Sioux Falls Rural with flat terrain | Immediately outside Anchorage Suburban | Inside Monterey, next to Monterey Regional Airport Suburban or urban | Suburban |
| Co-channel exclusion distance, long-term: [7] ([6] in brackets) for illustrative cases | 40 km (80 km) | 14 km (110 km) | 85 km (110 km) | 4 km |
| Co-channel exclusion distance, short-term | N/A | N/A | N/A | 10 km |

[a] Table numbers are from [6]

[b] Reference [6] uses ITM in area mode with $\Delta h$ equal to 10 m or 30 m, with clutter corrections 0-5 dB for suburban and 5-10 dB for urban conditions—much lower than our values. Reference [7] uses ITM in point-to-point mode with no clutter correction, meaning it assumes rural conditions.

the effect of increasing the antenna elevation for short-term protection to 20°.

*Adjacent channel selectivity.* Fig. 18, which plots data included in [6, Appendix A], shows that ACS can vary dramatically. Our baseline analysis uses the relatively wide ACS mask corresponding to Elmendorf AFB; for the sensitivity analysis, we also use the narrower ACS mask corresponding to FCDAS. The ACS only affects adjacent band

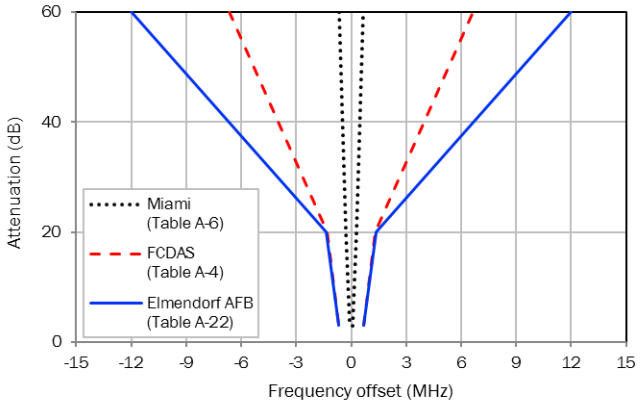


**FIGURE 18.** MetSat receiver selectivity for HRPT data at various locations (tables in [6]).

interference—it does not affect the co-channel interference or the calculated exclusion distance.

Fig. 19(a) shows the effect of the earth station antenna height and main beam gain on the combination of path loss and antenna gain at the mobile location. The results are based on the interfering transmitter being at the same azimuth as the antenna boresight (worst case). Fig. 19(b) gives similar results for changes in the earth station antenna elevation angle. These figures indicate a change of no more than 20 dB in the combination of propagation and antenna gain, based on an earth station antenna height of 55 m—much higher than the baseline. For comparison, different propagation models can give changes of more than 40 dB (Fig. 13(b)).

### D. OUT OF BAND EMITTERS

The characteristics of out of band emitters are difficult to quantify: they will vary according to the technology used, and are likely to change over time. Therefore, it is critical to address the major parameters through a sensitivity analysis.

The baseline analysis considers out of band emitters only in the nearest block (the AWS-1 A block), and assumes that the ACLR is uniformly distributed between 30 and 40 dB. In the sensitivity analysis, we vary both assumptions.

We consider out of band emitters in both the A and B blocks—doubling the number of emitters that contribute to OOBE interference. In this case, we retain the uniformly distributed exclusion losses.

We consider two further cases of exclusion losses. In place of the uniform distribution between 30 and 40 dB, we set all emitters to have 30 dB exclusion, and all to have 40 dB exclusion.

To a first approximation, both changes lead to a change of 3 to 5 dB in the aggregate interference power.

### E. ILLUSTRATIONS OF RESULTS

We present two figures to illustrate and clarify the results summarized in Table 8.

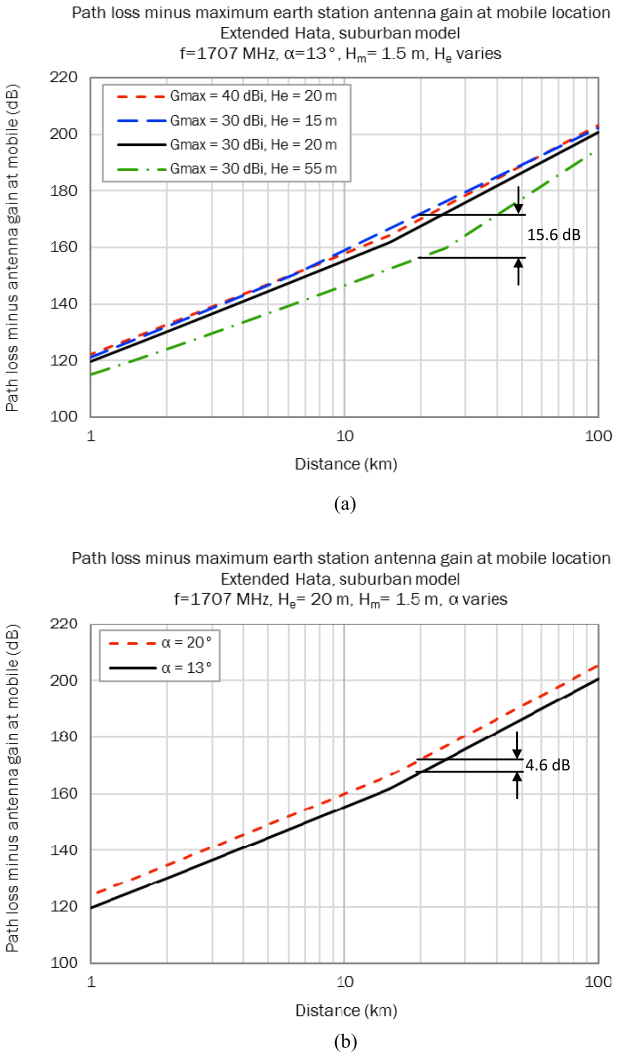


**FIGURE 19.** Combination of path loss and maximum earth station antenna gain at the mobile location as a function of distance, for different earth station antenna heights, main beam gains, and elevation angle. Maximum earth station antenna gain is based on the earth station antenna boresight azimuth being in the direction of the mobile.
(a) Variation with earth station antenna height and antenna gain.
(b) Variation with earth station antenna elevation angle.

Fig. 20 illustrates the baseline case. Fig. 20(a) shows three values associated with adjacent band transmitters: the aggregate interference power values associated with ABI and OOBE occurring 0.0125% of the time, and their sum.

Fig. 20(b) highlights three summary values:

- the aggregate interference power for ABI plus OOBE;
- the 10km exclusion distance based requiring that the co-channel aggregate interference power at 0.0125% not exceed the IPC;
- the 2km exclusion distance based on requiring that the co-channel aggregate interference power at 0.0125% not exceed the corresponding aggregate interference power due to adjacent band transmitters.

Fig. 21 illustrates the summary values for one of the cases in the sensitivity analysis—setting the standard deviation of location variability to 12 dB.

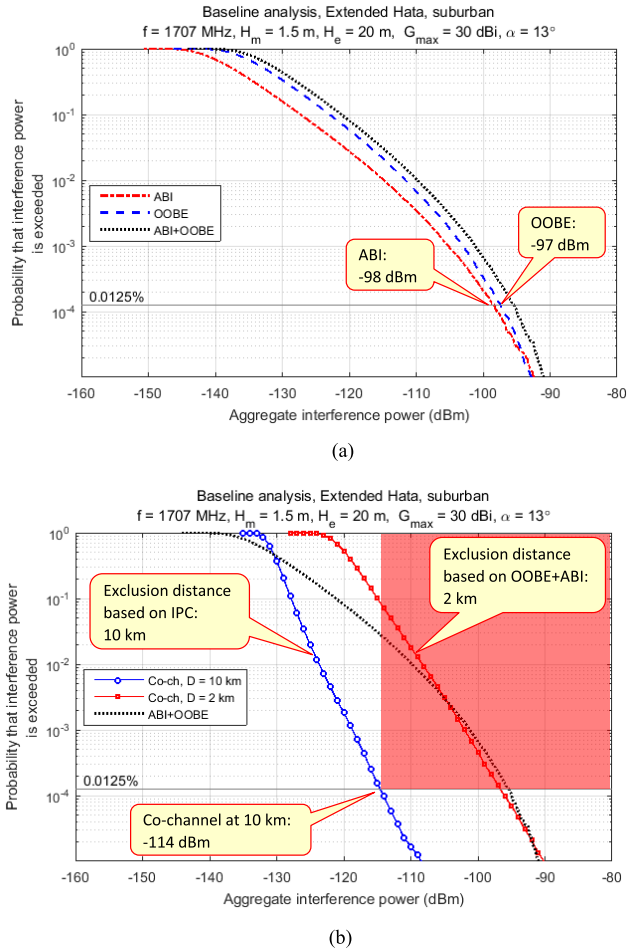


**FIGURE 20.** Illustration of the summary values used to present the results of the sensitivity analysis: baseline case. (a) Baseline risk chart for adjacent band transmitters showing the summary values presented in Table 8. The interference power for ABI and OOBE combined is used to assess the effects of co-channel interference, see (b). (b) Risk chart for co-channel transmitters showing the summary values presented in Table 8.

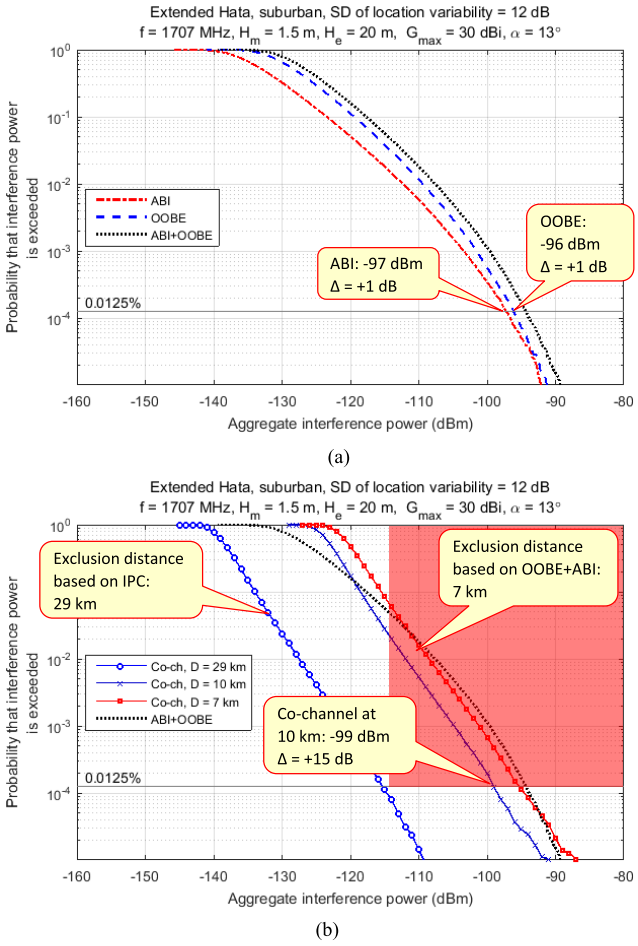


**FIGURE 21.** Illustration of the summary values used to present the results of the sensitivity analysis: in the case shown here, the standard deviation of the location variability is set to 12 dB. The Δ values are the changes in aggregate interference power compared to the baseline case. (a) Risk chart for adjacent band transmitters showing the summary values presented in Table 8 for cases in the sensitivity analysis. Δ is the change when going from 8 to 12 dB location variability. (b) Risk chart for co-channel transmitters showing the summary values presented in Table 8 for cases in the sensitivity analysis.

We show the interference power associated with ABI and OOBE occurring 0.0125% of the time in Fig. 21(a), together with the change Δ in these values compared to the baseline case (see Table 8). Similarly, for the co-channel interference (Fig. 21(b)), we show the change (Δ) in the co-channel aggregate interference power based on three exclusion distances: a standard 10-km distance; based on the IPC (29 km); and based on requiring that the co-channel aggregate interference power at 0.0125% not exceed the corresponding aggregate interference power due to adjacent band transmitters (7 km).

The short-term interference increases by $\Delta = 1$ dB for both OOBE and ABI, and by $\Delta = 15$ dB for co-channel interference at 10 km. The exclusion distance based on the IPC increases to 29 km; the exclusion distance at which the co-channel aggregate interference power matches the aggregate interference power due to adjacent band transmitters increases to 7 km.

## IX. CONCLUSIONS AND RECOMMENDATIONS

As systems pioneer George Box famously said, "Remember that all models are wrong; the practical question is how wrong do they have to be to not be useful" [33, p. 74]. While our model is clearly imperfect, we believe that it is still useful.

We conclude that risk-informed interference analysis can be successfully applied in a real-world case. Protection criteria that combine an interfering power level with statistical limits on how often it may be exceeded provide a straightforward and helpful set of criteria for a risk-informed interference assessment. While such protection criteria are already being used in a number of services, including the satellite service and broadcast protection contours, the more widespread use of statistical service rules will support future risk analysis.

Risk-based analysis yields useful insights. Our work shows that the binding constraint is not the long-term interference condition at 5° receiver antenna elevation assumed in prior

studies, but the short-term interference condition at 13°. The sensitivity analysis highlights the need to better characterize radio propagation, and particularly to update the understanding of clutter in urban and suburban environments—noting that current models rely on measurements taken in Japan in the 1960s [25]. Ongoing work by NTIA [34] will be very valuable.

The consequence metric used does not shed any light on the service quality impacts of non-interference hazards such as variations in desired signal power or operational problems. The development of criteria based on service metrics, such as bit-error ratios, would allow a more comprehensive analysis.

This analysis was limited by several factors. We could not find ITU-R material to enable the use of bit-error ratio metrics. Many of the parameter values in the ITUR documentation—which were developed for the satellite community by the satellite community—are stated without explanation or backup. Baseline system performance metrics were unavailable.

Moving forward, as risk-based interference studies are used more often in decision making, it is important to increase the transparency of the process and the analysis. The reproducibility, and even the credibility, of such analyses can be enormously increased through a combination of transparency (for example, by publishing any supporting calculations; see footnote 3) and open peer review.

## Acknowledgments

The authors are grateful to J. Dooley, E. Drocella, P. McKenna, I. Navarro, R. Pavlak, R. Peterson, J. Riihijärvi, and S. Sharkey for their help and insight. They thank an anonymous reviewer for detailed and useful feedback, and J. Ward-Bailey and M. Galvan for editing support.

## REFERENCES

[1] FCC TAC. (Apr. 2015). *FCC Technological Advisory Council, Spectrum, and Receiver Performance Working Group. A Quick Introduction to Risk-Informed Interference Assessment* [Online]. Available: http://transition.fcc.gov/bureaus/oet/tac/tacdocs/meeting4115/Intro-to-RIA-v100.pdf

[2] S. Kaplan and B. J. Garrick, "On the quantitative definition of risk," *Risk Anal.*, vol. 1, no. 1, pp. 11–27, Mar. 1981. [Online]. Available: http://dx.doi.org/10.1111/j.1539-6924.1981.tb01350.x

[3] J. P. De Vries, "Risk-Informed interference assessment: A quantitative basis for spectrum allocation decisions," in *Proc. Res. Conf. Commun. Inf. Internet Policy (TPRC)*, Washington, DC, USA, 2015. [Online]. Available: http://ssrn.com/abstract=2574459

[4] J. P. de Vries, "Risk-informed interference assessment: A quantitative basis for spectrum allocation decisions, telecommunications policy," 2017. [Online]. Available: http://dx.doi.org/10.1016/j.telpol.2016.12.007

[5] FCC TAC. (Dec. 2015). *A Case Study of Risk-Informed Interference Assessment: MetSat/LTE Coexistence in 1695-1710 MHz* FCC Technological Advisory Council, Spectrum, and Receiver Performance Working Group, [Online]. Available: https://transition.fcc.gov/bureaus/oet/tac/tacdocs/meeting121015/MetSat-LTE-v100-TAC-risk-assessment.pdf

[6] NTIA. *An Assessment of the Near-Term Viability of Accommodating Wireless Broadband Systems in the 1675-1710 MHz, MHz, 3500-3650 MHz, 4200-4220 MHz, and 4380-4400 MHz Bands*, U.S. Dept. Commerce, Washington, DC, USA, pp. 1755–1780, Oct. 2010. [Online]. Available: http://www.ntia.doc.gov/files/ntia/publications/fasttrackevaluation_11152010.pdf

[7] "Working group 1 final report-1695-1710 MHz meteorological-Satellite," Commerce Spectrum Manage. Advisory Committee, CSMAC, Washington, DC, USA, Tech. Rep., Jul. 2013. [Online]. Available: http://www.ntia.doc.gov/files/ntia/publications/wg1_report_07232013.pdf

[8] FCC. (Oct. 1, 2015). *Auction 97: Advanced Wireless Services (AWS 3)*. [Online]. Available: http://wireless.fcc.gov/auctions/default.htm/?job=auction_summary&id=97

[9] *Aggregate Interference Criteria for Space-to-Earth Data Transmission Systems Operating in the Earth Exploration-Satellite and Meteorological-Satellite Services Using Satellites in Low-Earth Orbit*, document ITU Radiocommun. Sector Rec. SA.1026-4, 2009. [Online]. Available: http://www.itu.int/rec/R-REC-SA.1026-4-200902-I/en

[10] NASA. (Apr. 8, 2013). *NOAA Polar-Orbiting Operational Environmental Satellite (POES)*. [Online]. Available: https://eosweb.larc.nasa.gov/ACEDOCS/data/appen.c.1.html

[11] J. P. Monteverdi. (2016). *Polar Orbiting Environmental Satellites (POES)*. [Online]. Available: http://tornado.sfsu.edu/geosciences/classes/m407_707/Monteverdi/Satellite/PolarOrbiter/Polar_Orbits.html

[12] NOAA. OSGS Sustain Mission. (2016). *Office of Systems Architecture and Advanced Planning* [Online]. Available: https://www.nesdis.noaa.gov/OSAAP/sustain.html

[13] FCC. (May 14, 2014). *AWS-3 Band Plans* [Online]. Available: http://wireless.fcc.gov/services/aws/data/AWS3bandplan.pdf

[14] *The Use of Short Term Probabilities in Interference Criteria Documents, With a Preliminary Draft Revision to Recommendation ITU-R SA. 1026-3*, USA Delegation, ITU Radiocommun. Study Groups, document 7B/159-E, Jan. 2007.

[15] E. F. Drocella *et al.*, "3.5 GHz exclusion zone analyses and methodology," U.S. Dept. Commerce, Washington, DC, USA, Tech. Rep. NTIA TR-15-517, Mar. 2016. [Online]. Available: http://www.its.bldrdoc.gov/publications/2805.aspx

[16] F. H. Sanders, R. L. Sole, B. L. Bedford, D. Franc, and T. Pawlowitz, "Effects of RF interference on radar receivers," U.S. Dept. Commerce NTIA, Washington, DC, USA, Tech. Rep. TR-06-444, Feb. 2006. [Online]. Available: http://www.its.bldrdoc.gov/publications/06-444.aspx

[17] NOAA. (Jan. 15, 2014). GOES Operational Status. *Office of Satellite and Product Operations*. [Online]. Available: http://www.ospo.noaa.gov/Operations/GOES/status.html

[18] NOAA. (Jan. 27, 2017). POES Operational Status. *Office of Satellite and Product Operations*. [Online]. Available: http://www.ospo.noaa.gov/Operations/POES/status.html

[19] *Working Document Toward a Preliminary Draft New Recommendation ITU-R SA. [EES/MET PERF]: MetSat and EESS Performance Objectives in The Presence of Interference*, USA Delegation, ITU Radiocommun. Study Groups, document ITU-R WP7B Contribution, Jun. 2010.

[20] *Methodology for Determining Interference Criteria for Systems in the Earth Exploration-Satellite and Meteorological-Satellite Services*, ITU Radiocommun. Sector Recommendation, document SA.1022-0 in SA.1022, 1994. [Online]. Available: https://www.itu.int/rec/R-REC-SA.1022-0-199403-S/en

[21] J. Riihijärvi, A. Achtzehn, P. Mahonen, and P. de Vries, "A study on the design space for harm claim thresholds," in *Proc. 9th Int. Conf. Cognit. Radio Oriented Wireless Netw. Commun. (CROWNCOM)*, Oulu, Finland, Jun. 2014, pp. 377–382.

[22] "LTE user equipment: Coexistence with 862-870MHz," Ofcom, London, U.K., Tech. Rep., Sep. 2012. [Online]. Available: http://stakeholders.ofcom.org.uk/binaries/consultations/award-800mhz/statement/lte-coexistence.pdf

[23] Committee on Improving Risk Analysis Approaches used by the U.S. EPA, National Research Council, *National Research Council, Science and Decisions: Advancing Risk Assessment*. Washington, DC, USA: National Academies Press, 2009. [Online]. Available: http://www.nap.edu/catalog/12209/

[24] G. A. Hufford, A. G. Longley, and W. A. Kissick, "A guide to the use of the ITS irregular terrain model in the area prediction mode," U.S. Dept. Commerce, Washington, DC, USA, Tech. Rep. NTIA 82-100, Apr. 1982.

[25] Y. Okumura, "Field strength and its variability in VHF and UHF land-mobile radio service," *Rev. Elect. Commun. Lab.*, vol. 16, nos. 9–10, Sep./Oct. 1968.

[26] M. Hata, "Empirical formula for propagation loss in land mobile radio services," *IEEE Trans. Veh. Technol., VT*, vol. 3, no. 3, pp. 317–325, Aug. 1980.
[27] A. G. Longley and P. L. Rice, "Prediction of tropospheric radio transmission loss over irregular terrain: A computer method-1968," U.S. Dept. Commerce, Washington, DC, USA, Tech. Rep. ERL 79-ITS 67, Jul. 1968.
[28] A. G. Longley and R. K. Reasoner, "Comparison of propagation measurements with predicted values in the 20 to 10,000 MHz range," U.S. Dept. Commerce, Washington, DC, USA, Tech. Rep. ERL 148-ITS 97, Jan. 1970.
[29] A. G. Longley and G. A. Hufford, "Sensor path loss measurements analysis and comparison with propagation models," U.S. Dept. Commerce, Washington, DC, USA, Tech. Rep. OT 75-74, Oct. 1975.
[30] A. G. Longley, "Radio propagation in urban areas," U.S. Dept. Commerce, Washington, DC, USA, Tech. Rep. OT 78-144, Apr. 1978, reissued Mar. 2016. [Online]. Available: http://www.its.bldrdoc.gov/publications/2674.aspx
[31] S. P. Tonkin, "A tutorial on the Hata and ITM propagation models: Confidence, reliability, and clutter with application to interference analysis," Tech. Rep., Jan. 2017. [Online]. Available: https://ssrn.com/abstract=2880916
[32] Council on Tall Buildings and Urban Habitat, "Tall buildings in numbers," *CTBUH J.*, vol. 2015 no. 2, pp. 52–53, Jun. 2015. [Online]. Available: http://global.ctbuh.org/resources/papers/2332-Journal2015_IssueII_TBIN.pdf
[33] G. E. P. Box and N. R. Draper, *Empirical Model-Building and Response Surfaces*, 1st ed. New York, NY, USA: Wiley, 1987.
[34] C. Hammerschmidt and R. Johnk, "Extracting clutter metrics from mobile propagation measurements in the 1755–1780 MHz band," in *Proc. IEEE Military Commun. Conf.*, Baltimore, MD, USA, Nov. 2016, pp. 213–218. [Online]. Available: http://www.its.bldrdoc.gov/publications/3166.aspx

**J. PIERRE DE VRIES** received the D.Phil. degree in theoretical physics from the University of Oxford, U.K., in 1987. He was with Microsoft Corporation in various roles, including the Senior Director of Advanced Technology and Policy. He has been a Senior Fellow and the Co-Director of the Spectrum Policy Initiative with the Silicon Flatirons Center, University of Colorado Boulder, Boulder, CO, USA, since 2011. His current work focuses on maximizing the value of radio operation, by improving allocation decisions, clarifying rights and responsibilities, and decentralizing spectrum management.

Dr. de Vries is a member of the FCC's Technological Advisory Council, and a Board Member of TPRC.

**URI LIVNAT** received the B.Sc. degree in electrical and computer engineering from Ben-Gurion University of the Negev, Israel, in 2009, and the M.S. degree in electrical engineering from Columbia University in 2014.

From 2009 to 2012, he was with Broadcom Corporation, Israel, as a Wireless Backhaul Engineer. In 2013, he joined the Office of Engineering and Technology, Federal Communication Commission (FCC), and also served as a Liaison and a Consultant for the FCC's Technological Advisory Council. His research, with AT&T's Research Department, focused on fair resource allocation for multiple users in a heterogeneous wireless networks environment. His honors and awards include the Dean's Fellowship for academic achievement in 2009 and the Nicola Tesla Scholarship in 2012.

**SUSAN P. TONKIN** received the D.Phil. degree in theoretical physics from the University of Oxford, U.K., in 1986, and the M.S. degree in coastal engineering from the University of Washington, USA, in 2001.

From 2001 to 2015, she was a Coastal Engineer with Moffatt & Nichol. As a member of the ASCE, she supported the development of structural design criteria for tsunami-resistant buildings. She has engaged in research in the areas of radar clutter and biological neural networks. Her current research is the application of statistical methods to engineering problems.